

# Electron MHD: dynamics and turbulence

Maxim Lyutikov

Department of Physics, Purdue University, 525  
Northwestern Avenue, West Lafayette, IN 47907-2036

and

The Canadian Institute for Theoretical Astrophysics, University of  
Toronto, 60 St. George Street Toronto, Ontario, M5S 3H8 Canada

We consider dynamics and turbulent interaction of whistler modes within the framework of inertialess electron MHD (EMHD). We argue there is no energy principle in EMHD: any stationary closed configuration is neutrally stable. On the other hand, the relaxation principle, the long term evolution of a weakly dissipative system towards Taylor-Beltrami state, remains valid in EMHD.

We consider the turbulent cascade of whistler modes. We show that (i) harmonic whistlers are exact non-linear solutions; (ii) co-linear whistlers do not interact (including counter-propagating); (iii) waves with the same value of the wave vector,  $k_1 = k_2$ , do not interact; (iv) whistler modes have a dispersion that allows a three-wave decay, including into a zero frequency mode; (v) the three-wave interaction effectively couples modes with highly different wave numbers and propagation angles. In addition, linear interaction of a whistler with a single zero-mode can lead to spatially divergent structures via parametric instability. All these properties are drastically different from MHD, so that the qualitative properties of the Alfvén turbulence cannot be transferred to the EMHD turbulence.

We derive the Hamiltonian formulation of EMHD, and using Bogolyubov transformation reduce it to the canonical form; we calculate the matrix elements for the three-wave interaction of whistlers. We solve numerically the kinetic equation and show that, generally, the EMHD cascade develops within a broad range of angles, while transiently it may show anisotropic, nearly two dimensional structures. Development of a cascade depends on the forcing (non-universal) and often fails to reach a steady state. Analytical estimates predict the spectrum of magnetic fluctuations for the quasi-isotropic cascade  $\propto k^{-2}$ . The cascade remains weak (not critically-balanced). The cascade is UV-local, while the infrared locality is weakly (logarithmically) violated.

## I. ELECTRON MHD

In this paper we consider the plasma dynamics in a specific range of parameters called the inertialess electron MHD, or just EMHD [1, 2]. This limit, by our definition, corresponds to time scales that are much shorter than ion dynamical time scales, but much longer than electron dynamical time scales. Thus, we consider the extreme limit, when the electrons are inertialess, while ions form a neutralizing background. This limit is qualitatively different from what is often called Hall MHD, which usually means MHD with a Hall term in the Ohm's law. The limit of inertialess electron MHD is, in some sense, not a smooth transition from MHD, since inertialess EMHD is not derived from a force balance, but from a constraint condition of zero electric field in the electron fluid frame, see below.

We have in mind two possible applications of the EMHD cascade (besides the accepted regimes of Solar wind and Earth magnetotail). First, in a weakly collisional astrophysical plasma the MHD cascade couples to the EMHD cascade at the ion gyro scale [3] (see, though Ref. [4]). Secondly, in the neutron star crusts ions form a neutralizing background, while electrons flow slowly, carrying a frozen-in magnetic field. Both cases have important applications, *e.g.*, for accreting flows around black holes and the behavior of strongly magnetized neutron stars, magnetars [5, 6].

We address a fundamental question: how does an arbitrary configuration EMHD evolve? This includes the question of stability, the way a perturbed system relaxes and the long term evolution. Typically, it is assumed that the EMHD system behaves similarly to the MHD. In this paper we argue that this is not the case: we demonstrate that any EMHD equilibrium is neutrally stable, so that the system evolves via non-linear wave interaction and forms a turbulent cascade. We then argue that the cascade remains weak (not critically balanced as in case of MHD), and propagates within a broad range of angle (not nearly two-dimensional).

## II. MAGNETIC FIELD DYNAMICS IN ELECTRON MHD

Within the framework of EMHD, the electric current is produced by the flow of electrons,  $\mathbf{J} = -nev$ , where  $n$ ,  $-e$ , and  $\mathbf{v}_e$  are the local number density, charge, and average velocity of the electrons [see, *e.g.*, Ref. 2, for derivation and limitations]. Ions provide a neutralizing background. In the limit of infinite conductivity, the electric field satisfies the condition,

$$\mathbf{E} + \mathbf{v}_e \times \mathbf{B} = 0, \quad (1)$$

which yields the induction equation

$$\frac{\partial \mathbf{B}}{\partial t} = \nabla \times (\mathbf{v}_e \times \mathbf{B}), \quad (2)$$

Replacing  $\mathbf{J} = -nev_e = \frac{c}{4\pi} \nabla \times \mathbf{B}$ , the only dynamical variable in this equation is the magnetic field [2]:

$$\frac{\partial \mathbf{B}}{\partial t} = -\frac{c}{4\pi e} \nabla \times \left( \frac{\nabla \times \mathbf{B}}{n} \times \mathbf{B} \right) \quad (3)$$

So, given an initial field configuration and appropriate boundary conditions, the induction equation uniquely determines its evolution. Importantly, *in the limit of inertialess EMHD, the plasma dynamics follows not from the force balance, but from a constraint condition (1).*

In what follows we consider the basic whistler interactions in the simplest case of constant rectilinear external magnetic field and constant density. Dimensionalizing EMHD equations by plasma and cyclotron frequency (so that time is measured in  $1/\omega_B$  and spacial coordinates in

terms of skin depth  $\delta = c/\omega_p$ ), absorbing factors of  $\sqrt{4\pi}$  into definition of electromagnetic fields, the EMHD equation (3) becomes.

$$\partial_t \mathbf{B} = -\nabla \times (\nabla \times \mathbf{B} \times \mathbf{B}) = ((\nabla \times \mathbf{B}) \cdot \nabla) \mathbf{B} - (\mathbf{B} \cdot \nabla) \nabla \times \mathbf{B} = Li_{\mathbf{B}}(\nabla \times \mathbf{B}) \quad (4)$$

Thus, the change of the magnetic field is associated with Lie-transport of the B-vector along the electron fluid with the current, and corresponding velocity  $-\nabla \times \mathbf{B}$ . Appearance of the Lie derivative in the temporal evolution is related to the fact that the EMHD equations can be written as a Hamiltonian system (see Section VI). Lie derivatives then is equivalent to the Poisson bracket [7].

### A. Waves in EMHD: fully non-linear whistlers

Let us assume that constant magnetic field  $\mathbf{B}_0 = B_0 \mathbf{e}_x$  is directed along  $x$  axis, and the wave is propagating at angle  $\theta$  with respect to the magnetic field. First, note that a harmonic wave of *arbitrary* amplitude  $\delta B$  is an exact solution of EMHD

$$\begin{aligned} \mathbf{B} &= B_0 \mathbf{e}_x + \delta B \mathbf{e}_B e^{-i(\omega t - k(x \cos \theta + z \sin \theta))} \\ \omega &= \mathbf{B}_0 k^2 |\cos \theta| \\ \mathbf{e}_B &= \frac{1}{2} \{-i \sin \theta, 1, i \cos \theta\} \end{aligned} \quad (5)$$

where  $\mathbf{e}_B$  is the eigenvector (regaining the constants,  $\omega = c^2 k^2 |\cos \theta| \omega_B / \omega_p^2$ ).

The whistler modes parametrized by (5) allow a universal treatment of the field-aligned and counter-aligned propagation, without a need to introduce separate polarization states [as, *e.g.*, done in Ref. 8].

The fact that an arbitrary amplitude harmonic wave is a solution of EMHD equation *does not mean* that an wave cannot experience a decay. Recall, in MHD an arbitrary Alfvén wave, not necessarily harmonic, is an exact solution for parallel propagation. In the case of EMHD, only harmonic waves are non-linear solutions. Two non-collinear harmonic waves will produce a third, beat wave. Or, reversely, a given wave can decay in two.

There are special cases when the strong whistler waves do not interact. Let us assume that there two fully non-linear modes with wave numbers  $k_1$  and  $k_2$  propagating at angles  $\theta_1$  and  $\theta_2$  (not necessarily co-planar). One can demonstrate by direct calculations that two fully non-linear harmonic waves are completely non-interacting for (i) co-linear propagation (including counter-propagating case); (ii) when the two modes have the same wave-vector  $k_1 = k_2$  (but propagating in different directions), see below Section VIII

An initial perturbation with a broad range of wave vectors can be represented as a sum of harmonic waves. For aligned propagation (so that the initial perturbation is not experiencing angular spreading) these waves are non-interacting, but since different modes have different velocities and initial perturbation will experience a dispersive spreading along the direction of propagation.

## III. CONSERVATION LAWS

Equations of EMHD conserve energy

$$\begin{aligned} \partial_t B^2 / 2 + \nabla \cdot (\mathbf{E} \times \mathbf{B}) &= 0 \\ \mathbf{E} &= \nabla \times \mathbf{B} \times \mathbf{B} = \mathbf{J} \times \mathbf{B} \\ \mathbf{E} \times \mathbf{B} &= (\nabla \times \mathbf{B} \cdot \mathbf{B}) \mathbf{B} - B^2 \nabla \times \mathbf{B} \end{aligned} \quad (6)$$

Note that the two terms in the Poynting flux separate energy transport by velocity  $v = -\nabla \times \mathbf{B}$  and parallel energy transport. The current flow is divergenceless as well:

$$\mathbf{J} = \nabla \times \mathbf{B}, \nabla \cdot \mathbf{J} = 0 \quad (7)$$

The equations of EMHD cannot be written in fully conservative form (as a divergence of the stress-energy tensor), since the force balance is not included in the EMHD formulation: there are tensile forces that balance Lorentz force  $\mathbf{J} \times \mathbf{B}$ , but those forces do no work,  $\mathbf{v} \cdot \mathbf{J} \times \mathbf{B} = 0$ , so that energy is conserved.

In EMHD the helicity is conserved:

$$\begin{aligned} \partial_t(\mathbf{A} \cdot \mathbf{B}) &= (\mathbf{B} \cdot \nabla)f - \mathbf{A} \cdot \nabla \times (\mathbf{J} \times \mathbf{B}) = (\mathbf{B} \cdot \nabla)f + \nabla \cdot (\mathbf{A} \times (\mathbf{J} \times \mathbf{B})) \\ \int dV \partial_t(\mathbf{A} \cdot \mathbf{B}) &= \int dV (\mathbf{B} \cdot \nabla)f + \int d\mathbf{S} \cdot (\mathbf{A} \times (\mathbf{J} \times \mathbf{B})) \end{aligned} \quad (8)$$

$$\int dV (\mathbf{B} \cdot \nabla)f = \int dV (\nabla(f\mathbf{B}) - f\nabla\mathbf{B}) = \int f\mathbf{B} \cdot d\mathbf{S} = 0 \quad (9)$$

So a change of helicity in a volume is due to flux of  $-\mathbf{A} \times \mathbf{J} \times \mathbf{B}$  through the surface. It is zero if  $\mathbf{n} \cdot \mathbf{B} = \mathbf{n} \cdot \mathbf{J} = 0$ , no magnetic field or current penetration through the surface.

In a differential form the conservation of helicity can be written as a conservation of the topological torsion four-vector.

$$\partial_t(\mathbf{A} \cdot \mathbf{B}) = -\nabla \cdot (\mathbf{A} \times \dot{\mathbf{A}}) \quad (10)$$

Though the condition  $\mathbf{n} \cdot \mathbf{J} = 0$  on the boundary seems to be an additional constraint in EMHD if compared with MHD, in fact, it is not: just like in ideal MHD the boundary must move with the flow, in ideal EMHD the boundary must move with the current, so no current actually crosses the boundary.

#### IV. THE ENERGY AND THE RELAXATION PRINCIPLES IN EMHD

In MHD the energy principle [9] and the relaxation principle [10, 11] play the most important role, allowing one to decide on a stability of a plasma configuration and its long term evolution without doing a full normal mode analysis. The energy principle allows one to decide on the stability of a particular stationary configuration by calculating an energy change induced by small perturbations: if the energy increase, then the configuration is linearly stable. The relaxation principle addresses the long term evolution of a system. In a viscous but electrically ideal MHD system, by dissipating the energy yet conserving the topology, the plasma tries to relax to the maximally twisted state, the force-free Woltjer-Taylor state. Somewhat similarly, in a weakly resistive medium magnetic energy cascades to smaller scales where dissipation is important, while helicity concentrates on larger scales and is thus better conserved.

As we show below, the case of EMHD is qualitatively different from MHD: there is no energy principle in EMHD. Recall, in MHD any stationary *closed* state is the result of the force balance. Conservative forces can be expressed as gradients of the corresponding potentials. Then the stable equilibria correspond to minima of the potential energy. The crucial ingredient in the energy principle is the fact that *the energy of a closed system can change due to internal motions*. Indeed, in MHD a work of Lorentz force is generally not zero,  $\int dV \mathbf{v} \cdot \mathbf{J} \times \mathbf{B} \neq 0$ . This is *not* true in EMHD: the work of the Lorentz force is identically zero,

$$\mathbf{v} \cdot \mathbf{J} \times \mathbf{B} \propto \mathbf{J} \cdot \mathbf{J} \times \mathbf{B} = 0. \quad (11)$$

Thus, the energy of a closed EMHD plasma cannot change. This immediately implies the absence of the energy principle, which *requires* that the magnetic energy tries to reach a minimal energy state. As another way to understand the absence of the relaxation principle in EMHD, recall that the equations of ideal EMHD are derived from the constant equation (that the electric field in the frame of the electron fluid is zero), and *not* from the force balance equation, like, *e.g.*, the MHD equations.

### A. Any closed EMHD equilibrium is neutrally stable

Mathematically, to prove the absence of the energy principle, let us prove that *any* stable configuration of EMHD plasma with constant plasma density has purely real frequency: it is neutrally stable. Let  $B_0$  be a stationary solution of Eq. (4),  $\partial_t \mathbf{B}_0 = 0$ . Let us consider an incompressible electron fluid perturbation  $\xi(\mathbf{r})$ , so that the perturbed magnetic field is

$$\delta \mathbf{B} = \nabla \times (\xi \times \mathbf{B}_0) = \mathcal{L}_{i\mathbf{B}_0} \xi \quad (12)$$

We find

$$\begin{aligned} \dot{\xi} \times \mathbf{B}_0 + \delta \mathbf{F} &= 0 \\ \delta \mathbf{F} &= \mathbf{J}_0 \times \delta \mathbf{B} + \delta \mathbf{J} \times B_0 \end{aligned} \quad (13)$$

It is well known that operator  $\delta \mathbf{F}(\xi)$  is self-adjoint [12]. For harmonic time variation  $\propto e^{-i\omega t}$  we find

$$\int dV \eta^* \cdot \dot{\xi} \times \mathbf{B}_0 = -i\omega \int dV \eta^* \cdot \xi \times \mathbf{B}_0 = i\omega \int dV \xi \cdot \eta^* \times B_0 \quad (14)$$

On the other hand, using self-adjointness of  $\mathbf{F}$ :

$$\int dV \eta^* \cdot \dot{\xi} \times \mathbf{B}_0 = - \int dV \eta^* \cdot \mathbf{F}(\xi) = - \int dV \xi \cdot \mathbf{F}(\eta^*) = \int dV \xi \cdot \dot{\eta}^* \times \mathbf{B}_0 = i\omega^* \int dV \xi \cdot \eta^* \times \mathbf{B}_0 \quad (15)$$

Comparing Eqns (14) and (15) we conclude that  $\omega = \omega^*$ , that is,  $\omega$  is purely real. This demonstrates that *any* stationary configuration of EMHD is neutrally stable to linear perturbations.

In fact, one can demonstrate the non-linear stability of an arbitrary EMHD equilibrium, not necessarily a closed one. By the Poynting theorem, Eq. (6), the energy within a volume can only change due to flow of energy through the boundary. (Again, this is qualitatively different from MHD, where magnetic field energy can change due to internal motion within a confined volume.) Consider harmonic perturbations of a given EMHD equilibrium  $\mathbf{B}_0$ . Generally, there will be two types of perturbations: those that do excite surface motion and those that do not. (Note, that the electron fluid element displacements at the star surface does not imply crustal motions.) If the outside medium is vacuum, the perturbations that do excite harmonic in time surface motion will be radiated away as electromagnetic Poynting flux (with local intensity  $B_n^2 \xi^2 \omega^2 / c$  where  $\xi$  is the amplitude of the electron fluid motion and  $B_n$  is the normal component of magnetic field). Perturbations that do not excite surface electron motion remain neutrally stable. Thus, *any* EMHD configuration is neutrally stable. Neutrally stability implies that none of the stable configurations work as attractors.

The above result, *i.e.*, the absence of the energy principle in EMHD, demonstrates that conditions for MHD stability cannot be directly applied to the EMHD stability, and many fundamental results has to be abandoned. For example, it is well known that in MHD purely toroidal or purely poloidal configurations are unstable. This is not true in EMHD: there can be neutrally stable purely toroidal and purely poloidal configurations!

Let us summarize. An EMHD stable state is qualitatively different from the MHD stable state. If a stable MHD state is perturbed, then according to the energy principle the new state has a higher energy, so a system tries to relax to the preferred stable state. If an EMHD stable state is perturbed, the system does not relax back to this state

## B. Relaxation principle

The energy principle discussed above addresses the short time scale evolution of a system. On the other hand, in MHD a different principle, the relaxation principle [10, 11], addresses the long term evolution of the MHD system. The relaxation principle tries to predict, without detailed calculations the long term evolution of a system. Topological constraints, like conservation of helicity, restrict a set of final states. The relaxation principle of MHD [10, 11] then states that an arbitrary MHD state first relaxes to a minimal energy state that has the same helicity as the initial state. In electrically ideal plasma the helicity is conserved exactly, while the energy can be dissipated via fluid viscous effects. In a weakly resistive plasma, helicity is concentrated on largest scales and thus is dissipated slower than the magnetic energy.

Since EMHD conserves helicity, the Taylor relaxation principle remains valid in EMHD as well: if an EMHD state is perturbed, the energy will cascade down to small scales, while helicity will be concentrated on largest scales. But the largest scales will have very little energy. In reality, the pure Taylor-Beltrami state [13] is not achievable due to realistic boundary conditions.

## V. MHD AND EMHD TURBULENCE: THE KEY DIFFERENCES

After the initial ideas on the MHD turbulence were laid out in Ref. [14] and [15], the modern theory of MHD turbulence is based on the Goldreich-Sridhar model [16–18], whereby the turbulence is described in terms of interacting, counter-propagating wave packets. The four-wave processes dominate, but three wave process, when one of the mode has zero frequency, also contribute to the cascade [18–21]. Interaction is local in  $k$ -space (so that only waves with similar wave numbers interact), leading to Kolmogorov-like cascade. The cascade is anisotropic [possibly even 3D anisotropic, 22], but the parallel and perpendicular scales are related to each other via the critical balance assumption.

Currently, the dominant view is that the development of the EMHD turbulence proceeds similarly to the MHD cascade, *i.e.*, that the turbulence becomes strong and as a result achieves a critical balanced state. The scaling of EMHD cascade was proposed to be either  $7/3$  [8, 23–26] or  $8/3$  [27]. The origin of these models, and the  $7/3$  scaling can be traced back to the Ref. [23]. Briefly, the frequency of vortex breaking at scale  $1/k$  is  $\nu_k \sim B_k k^2$  (from the EMHD equation (3)); assumption of constant energy flux in  $k$  space implies  $B_k^2 \nu_k = \text{const}$ , so that  $B_k \propto k^{-2/3}$ . The spectrum is then  $E_k \sim B_k^2/k \propto k^{-7/3}$ .

The work in Ref. [23] was criticized in Refs. [2, 6], where it was argued that the EMHD turbulence always remains weak. (This criticism also applies to later works that used the scaling of Ref. [23], [24] and others). Rephrasing the works [2, 6], in Ref. [23] it was assumed that the whistler mode interaction is based on a concept of a vortex, a long-lived coherent structure. Due to highly dispersive nature of the whistler modes, an initial packet with a spread  $\Delta k \sim k$ , will have phases mixed on time scale  $t_{mix} \sim 1/(kv_p) \sim 1/\omega$ . That is, a coherent vortex, or a wave package, falls apart on its own on its dynamical time without transferring energy to smaller scale, so that a concept of a vortex is inconsistent with its suggested life time. Thus, the period of whistlers at scale  $k$  is smaller than the inferred life time of a vortex by  $B_k/B_0$ . The non-linear interaction time is then longer by  $B_0/B_k$ ; the constancy of energy flux in the  $k$  space then implies  $B_k \propto k^{-1/2}$ ,

$E_k \propto k^{-2}$  [6]. This implies that EMHD cascade proceeds in the weak regime. Our numerical calculations, generally, confirm the picture suggested in Ref. [2, 6]:  $E_k \propto k^{-2}$  spectrum follows from the form of the matrix element, while the resulting cascade remains weak.

Another important issue related to the structure of the cascade is its anisotropy. Below in Section X we show that often the whistler cascade becomes quasi-isotropic, while generically highly anisotropic structures can appear transiently.

## VI. HAMILTONIAN FORMULATION OF EMHD AND THE THREE-WAVE INTERACTION MATRIX

Turbulent processes are best described in the Hamiltonian formulation [28]. In this section we derive the Hamiltonian formulation of EMHD and use it to derive the EMHD three-wave interaction matrix. Note, that in the conventional Hamiltonian formulation of MHD the velocity (or velocity potential) is an independent variable [28]. In contrast, in EMHD velocity is not an independent variable; this requires a different Hamiltonian formation, a different set of canonical variable.

Non-linear wave-wave interaction is usually considered in the occupation representation of mode excitation [28, 29]. As an elementary mode we take

$$\begin{aligned}\delta\mathbf{B} &= b\sqrt{\omega}\mathbf{e}_B e^{-i\Phi} \\ \mathbf{e}_B &= \frac{1}{2}\{-i\sin\theta, \cos\phi + i\cos\theta\sin\phi, i\cos\theta\cos\phi - \sin\phi\} \\ \Phi &= \omega t - \mathbf{k} \cdot \mathbf{r}\end{aligned}\tag{16}$$

where  $b$  is the mode amplitude, which corresponds to the creation operator in quantum mechanics. The angular variables are spherical coordinates of the wave vector in the frame aligned with magnetic field. This choice of variables  $b$  effectively accomplishes the Bogolyubov transformation [30], so that in the absence of interactions

$$\partial_t b(\mathbf{k}, t) + i\omega b(\mathbf{k}, t) = 0,\tag{17}$$

while the energy of the waves takes the canonical form

$$\mathcal{H} = \sum_k \omega_k b_k b_k^*\tag{18}$$

In these variables the linearized equations of motion become trivial, so that all the linear dynamic is incorporated into the dispersion relation  $\omega(\mathbf{k})$ .

The Lagrangian of EMHD includes the magnetic field energy density and a constraint equation (4). Let us chose  $\mathbf{B}$  as an independent coordinate (another choice is the vector potential); adding a constraint with a Lagrangian multiplier, the EMHD Lagrangian is

$$\mathcal{L} = -B^2/2 + \mathbf{S} \cdot (\dot{\mathbf{B}} + \nabla \times (\mathbf{J} \times \mathbf{B}))\tag{19}$$

Requirement of the stationary action is expressed in terms of the generalized Euler-Lagrange equation [31]

$$\frac{\delta\mathcal{L}}{\delta B_i} - \partial_t \left( \frac{\delta\mathcal{L}}{\delta \dot{B}_i} \right) - \nabla_k \left( \frac{\delta\mathcal{L}}{\delta B_{i,k}} \right) = 0.\tag{20}$$

This gives the dynamical equation for the Lagrange multiplier  $\mathbf{S}$ , which becomes the canonically conjugate variable to  $\mathbf{B}$ .

$$\begin{aligned}\frac{\delta\mathcal{L}}{\delta B_i} &= -\mathbf{B} + (\nabla \times \mathbf{S} \times \nabla \times \mathbf{B}) \\ \partial_t \left( \frac{\delta\mathcal{L}}{\delta \dot{B}_i} \right) &= \dot{\mathbf{S}} \\ \nabla_k \left( \frac{\delta\mathcal{L}}{\delta B_{i,k}} \right) &= \nabla \times (\mathbf{B} \times \nabla \times \mathbf{S})\end{aligned}\quad (21)$$

$$\dot{\mathbf{S}} = -\mathbf{B} + (\nabla \times \mathbf{S} \times \nabla \times \mathbf{B}) + \nabla \times (\mathbf{B} \times \nabla \times \mathbf{S}) \quad (22)$$

The Hamiltonian is then

$$\mathcal{H} = \mathbf{S} \cdot \dot{\mathbf{B}} - \mathcal{L} = B^2/2 - (\nabla \times (\nabla \times \mathbf{B} \times \mathbf{B})) \cdot \mathbf{S} \quad (23)$$

Following our observation above, Eq. (16), we first do the Fourier transform, then canonical transformations  $\mathbf{B} \rightarrow \sqrt{\omega}\mathbf{B}$ ,  $\mathbf{S} \rightarrow \mathbf{S}/\sqrt{\omega}$ , and then change to complex variables

$$\begin{aligned}\mathbf{b} &= (\mathbf{B} + i\mathbf{S})/\sqrt{2}, \quad \mathbf{b}^* = (\mathbf{B} - i\mathbf{S})/\sqrt{2} \\ \mathbf{B} &= \frac{\mathbf{b} + \mathbf{b}^*}{\sqrt{2}}, \quad \mathbf{S} = i\frac{\mathbf{b}^* - \mathbf{b}}{\sqrt{2}}\end{aligned}\quad (24)$$

with the equations of motion

$$\begin{aligned}\partial_t \mathbf{b} &= -i\frac{\delta\mathcal{H}}{\delta \mathbf{b}^*} \\ \partial_t \mathbf{b}^* &= i\frac{\delta\mathcal{H}}{\delta \mathbf{b}}\end{aligned}\quad (25)$$

In the new variables the Hamiltonian takes the form

$$\begin{aligned}\mathcal{H} &= \mathcal{H}_0 + \mathcal{H}_{int} \\ \mathcal{H}_0 &= \omega_k b_k b_k^* \\ \mathcal{H}_{int} &= \int d\mathbf{k}_1 d\mathbf{k}_2 \left( \frac{1}{2} V_{k \leftrightarrow 1,2} b^* b_1 b_2 \delta(\mathbf{k} - \mathbf{k}_1 - \mathbf{k}_2) + V_{1 \leftrightarrow k,2}^* b b_1 b_2^* \delta(\mathbf{k}_1 - \mathbf{k} - \mathbf{k}_2) \right) \\ V_{k \leftrightarrow 1,2} &= \sqrt{\frac{\omega_1 \omega_2}{\omega}} \{ \mathbf{e}_B^* \cdot [(\mathbf{k}_1 \times \mathbf{e}_{B_1}) \cdot \mathbf{k}_2] \mathbf{e}_{B_2} - (\mathbf{k}_2 \cdot \mathbf{e}_{B_1})(\mathbf{k}_2 \times \mathbf{e}_{B_2}) + (1 \leftrightarrow 2) \}\end{aligned}\quad (26)$$

## VII. THE THREE-WAVE RESONANT CONDITION FOR WHISTLERS

Two ingredients are important for the wave-wave interaction: the resonant condition that relates kinematically the properties of the participating waves and the interaction matrix, that determines the strength of the interaction. Let us first study the resonant condition.

The normal modes of EMHD, whistlers, have a dispersion relation of the decaying type, which resembles shallow water waves. Thus, in the weak turbulence regime we expect that 3-wave processes are the dominant. The three-wave resonant condition  $\delta(\mathbf{k}_0 - \mathbf{k}_1 - \mathbf{k}_2)\delta(\omega_0 - \omega_1 - \omega_2)$  for whistler waves reads

$$\begin{aligned}\omega_n &= k_n^2 |\cos \theta_n|, \quad n = 0, 1, 2 \\ \omega &= \omega_1 + \omega_2 \\ k \cos \theta &= k_1 \cos \theta_1 + k_2 \cos \theta_2 \\ k \sin \theta \sin \phi &= k_1 \sin \theta_1 \sin \phi_1 + k_2 \sin \theta_2 \sin \phi_2 \\ k \sin \theta \cos \phi &= k_1 \sin \theta_1 \cos \phi_1 + k_2 \sin \theta_2 \cos \phi_2\end{aligned}\quad (27)$$



(below we drop subscript 0 on the parent wave,  $k \equiv k_0$ ).

The resonant conditions can be resolved for  $\{k, \theta, \phi\}$  :

$$\begin{aligned}\cos \theta &= \frac{(k_1 \cos \theta_1 + k_2 \cos \theta_2)^2}{k_1^2 |\cos \theta_1| + k_2^2 |\cos \theta_2|} \\ k &= \frac{k_1^2 |\cos \theta_1| + k_2^2 |\cos \theta_2|}{k_1 \cos \theta_1 + k_2 \cos \theta_2} \\ \tan \phi &= \frac{k_1 \sin \theta_1 \sin \phi_1 + k_2 \sin \theta_2 \sin \phi_2}{k_1 \sin \theta_1 \cos \phi_1 + k_2 \sin \theta_2 \cos \phi_2}\end{aligned}\quad (28)$$

### A. Co-planar wave interaction

General resonance condition (27-28) is complicated; let us gain some insight into the non-linear wave interaction by considering a special cases, a decay (and a merger of) into co-planar (with magnetic field) propagating modes. As we discuss below, even this simple case is very complicated. First we consider wave decay,  $k; 1, 2$  processes (the semicolon separates the parent wave from the daughter waves). Later, in Section VII B, we consider the resonant conditions for wave confluence  $k; 1, 2$ .

#### 1. Co-planar decay of obliquely propagating waves

Setting  $\phi_i = 0$  and eliminating  $k_1, k_2$  from (27), one can derive the following relation between the angles of the waves:

$$|\cos \theta| \sin^2(\theta_1 - \theta_2) = |\cos \theta_1| \sin^2(\theta - \theta_2) + |\cos \theta_2| \sin^2(\theta - \theta_1) \quad (29)$$

Alternatively, eliminating  $\{k_2, \theta_2\}$  from the momentum conservation,

$$\begin{aligned}k_2 &= \sqrt{k^2 + k_1^2 - 2kk_1 \cos(\theta - \theta_1)} \\ \cos \theta_2 &= \pm \frac{k \cos \theta - k_1 \cos \theta_1}{\sqrt{k^2 + k_1^2 - 2kk_1 \cos(\theta - \theta_1)}},\end{aligned}\quad (30)$$

one can derive the following resonance condition

$$k^2 \cos \theta = k_1^2 |\cos \theta_1| + \sqrt{k^2 + k_1^2 + 2kk_1 \cos(\theta - \theta_1)} |k \cos \theta - k_1 \cos \theta_1| \quad (31)$$

For given properties of the parent wave  $\{k, \theta\}$ , Eq. (31) is an equation for  $k_1(\theta_1)$  (it is also an equation for  $k_2(\theta_2)$  after a substitution  $k_1 \rightarrow k_2$ ,  $\theta_1 \rightarrow \theta_2$ .) Its solution is

$$\begin{aligned}k_1 &= (\cos^2 \theta + 2 \cos \theta \cos \theta_1 + 4 \cos \theta \cos(\theta - \theta_1) \cos \theta_1 + \cos^2 \theta_1 \pm \\ &(\cos \theta - \cos \theta_1) \sqrt{\cos^2 \theta + 2 \cos \theta (3 - 4 \cos(\theta - \theta_1) \cos \theta_1 + \cos^2 \theta_1)}) \frac{k}{2(3 \cos \theta + \cos(\theta - 2\theta_1)) \cos \theta_1}\end{aligned}\quad (32)$$

see Fig. (1). For a given  $\{k, \theta\}$  the angle  $\theta_1$  can be chosen to lie in the range  $-\pi/2 < \theta_1 < \pi/2$ . The resonance condition will then give  $\{k_2, \theta_2\}$  that generally may be propagating opposite to the initial wave,  $\theta_2 > \pi/2$ . For a simple decay, the wave vector of the daughter mode  $k_1$  can be up to two times larger than  $k$ ,  $k_1 \rightarrow 2k$  for  $\theta, \theta_1 \rightarrow \pi/2$ .

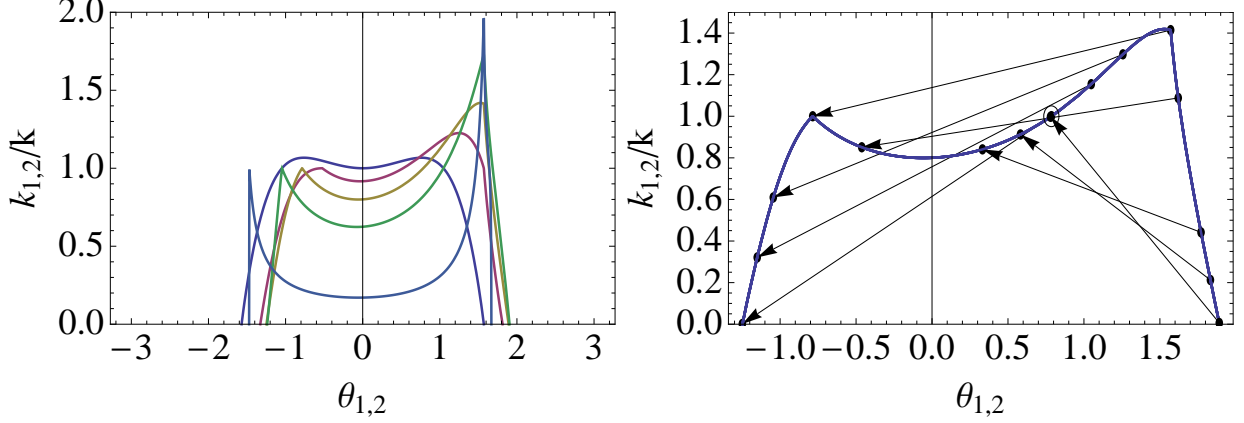


FIG. 1. *Left Panel.* Dispersion relation for the decay modes  $\{k_1, \theta_1\}, \{k_2, \theta_2\}$ , oblique propagation of the parent-wave,  $\theta = 0, \pi/6, \pi/4, \pi/3, \pi/2 - 0.1$  (becoming more peaked at  $\theta_{1,2} = \pi/2$  for higher initial angles). The maximal wave number for daughter wave is  $2k$ , reached for a highly oblique parent mode. Negative values of  $\theta$  indicate emission of a wave propagating in the direction opposite to the parent mode along the  $y$  axis. *Right Panel.* Pairing of the two daughter modes,  $\theta = \pi/4$ .

General relations take especially simple form for the parent wave propagating along magnetic field:

$$k_{1,2} = \frac{1 + 2 \cos \theta_{1,2} + 5 \cos^2 \theta_{1,2} + (1 - \cos \theta_{1,2})^{3/2} \sqrt{1 + 7 \cos \theta_{1,2}}}{4 \cos \theta_{1,2} (1 + \cos^2 \theta_{1,2})} k, \quad (33)$$

see Fig 2. The dispersions curve in Fig. 2 implies that a whistler mode propagating along magnetic field can decay only into two forward propagating waves. For parallel propagating parent wave the angles of the two daughter modes are related via

$$\cos \theta_2 = \frac{1 + (2 - 3 \cos \theta_1) \cos \theta_1 + \sqrt{1 - \cos \theta_1} (1 + \cos \theta_1) \sqrt{1 + 7 \cos \theta_1}}{2 + 6 \cos \theta_1 + \cos^2 \theta_1}, \quad (34)$$

see Fig. 2.

One of the daughter modes has  $\{k_1 < k, \theta_1 > \pi/3\}$ , another  $\{k_2 > k, \theta_2 < \pi/3\}$ . The maximal wave number is reached at  $\theta_2 = 0.76$  and is equal to  $k_2 = 1.06k$ . Note, that for the inverse process, a merger of two waves, *in order to create a whistler propagating along magnetic field with wave number  $k$ , one of the waves should have  $k_1 > k$* . As a special case, there is kinematically allowed decay of  $\{k, \theta = 0\}$  mode into two modes  $\{k, \theta = \pi/3\}$ , (daughter modes have the same  $k$  as the initial wave). As we discuss in Section II A, such process actually does not occur (zero matrix element).

Let us highlight a number of important features. (i) If the parent mode propagates at angle  $\theta$ , one of the daughter modes has  $\theta_1 > \theta$ . For  $\theta < \theta_1 < \pi/2$ , the other wave has  $-\pi/2 < \theta_2 < -\theta$ . (ii) obliquely propagating mode can decay into backward moving wave,  $\theta_1 > \pi/2$ . The maximal angle for a backward propagating wave is  $\theta_{1,max} = \pi/2 + \arccos(4\sqrt{3}/7)$ ; it is reached for  $\theta = \pi/3$ , in this case  $\theta_2(\theta_{1,max}, \theta = \pi/3) = 0$ . For  $\theta > \pi/3$  and  $\theta_1 > \pi/2$ , both product waves propagate in the same direction along  $y$  axis,  $\theta_2 > 0$ . As  $\theta_2 \rightarrow \theta - 0$ ,  $\theta_1 \rightarrow \pi/2 + 0$ . (iii) All the daughter modes have  $k_{\parallel;1,2} < k_{\parallel}$ , Fig. 4.

## B. Confluence of waves, $1; k, 2$

In addition to the  $k; 1, 2$  interaction, the kinetic equation (38) also involves the  $1; k, 2$  resonance. Now the two daughter modes  $1, 2$  are not interchangeable. The  $1; k, 2$  resonance is more compli-

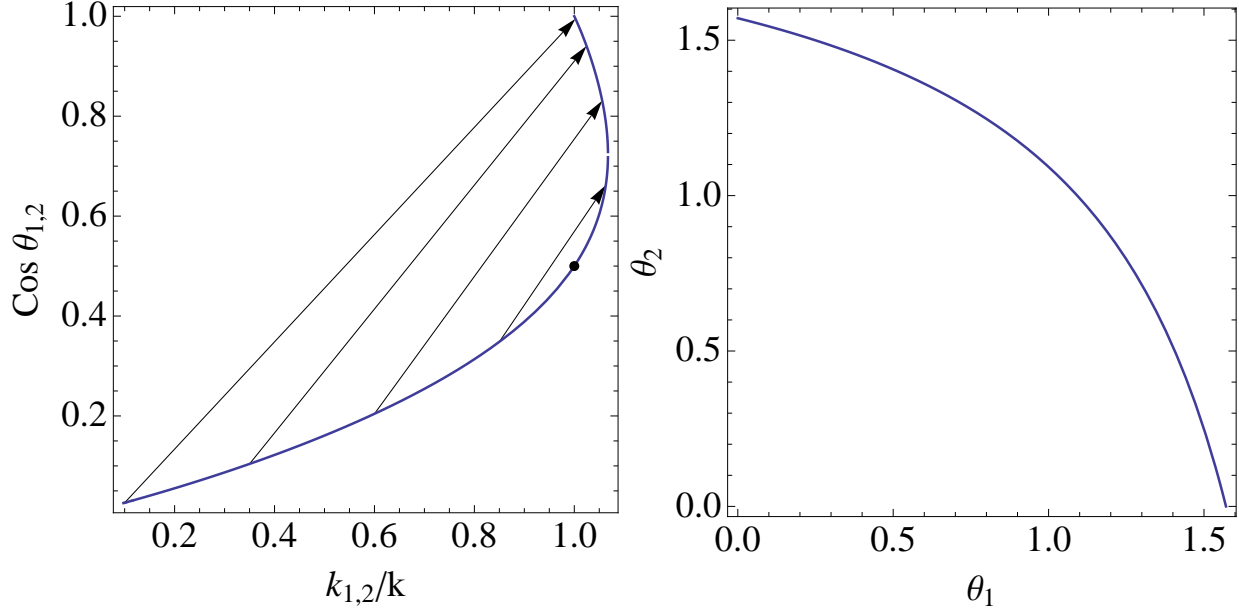


FIG. 2. *Left Panel.* Dispersion relation for the decay modes  $\{k_1, \theta_1\}, \{k_2, \theta_2\}$ , parallel propagation of the parent-wave. Arrows connect the two decay product waves. The small dot separates the two product waves. Two daughter modes propagate in the opposite direction along  $y$  axis. *Right Panel.* Relation between the angles of the two daughter modes for a decay of a parallel-propagating initial mode (absolute values of  $\theta_1$  and  $\theta_2$  are plotted).

cated, Fig. 5. Fig. 5 illustrates that the 3-waves processes couple modes with very different  $k$  and  $\theta$ :

The complications of the resonant conditions for  $\theta \rightarrow \pi/2$  make even the kinetic calculations very challenging: the resonant conditions change drastically on scales of  $\sim$  hundredth of a radian. At the same time the resonant wave vectors vary, basically from zero to infinity. To take correct account of these factors requires high resolution in both  $\theta$  and  $k$ .

## VIII. NON-LINEAR INTERACTION OF WHISTLERS, WAVE KINETIC EQUATION AND KOLMOGOROV-LIKE SPECTRUM

### A. Weak interaction of whistlers

Following the weak turbulence approach, we assume that the wave amplitude  $b$  is a slowly varying function of time,  $b(\epsilon t)$ , where  $\epsilon \ll 1$  is the wave amplitude expansion parameter. Using the EMHD equation as a Lie derivative of magnetic field along the current, Eq. (4), multiplying by  $\mathbf{e}_B^*$ , and expanding in  $\epsilon$

$$\begin{aligned}
 \partial_t b_{\mathbf{k}} &= \frac{\delta \mathcal{H}_{int}}{\delta b_{\mathbf{k}}^*} \\
 \mathcal{H}_{int} &= \int d\mathbf{k}_1 d\mathbf{k}_2 \left( \frac{1}{2} V_{k \leftrightarrow 1,2} b^* b_1 b_2 \delta(\mathbf{k} - \mathbf{k}_1 - \mathbf{k}_2) + V_{1 \leftrightarrow k,2} b b_1 b_2^* \delta(\mathbf{k}_1 - \mathbf{k} - \mathbf{k}_2) \right) \\
 V_{k \leftrightarrow 1,2} &= \sqrt{\frac{\omega_1 \omega_2}{\omega}} \{ \mathbf{e}_B^* \cdot [(\mathbf{k}_1 \times \mathbf{e}_{B_1}) \cdot \mathbf{k}_2] \mathbf{e}_{B_2} - (\mathbf{k}_2 \cdot \mathbf{e}_{B_1})(\mathbf{k}_2 \times \mathbf{e}_{B_2}) + (1 \leftrightarrow 2) \} \quad (35)
 \end{aligned}$$

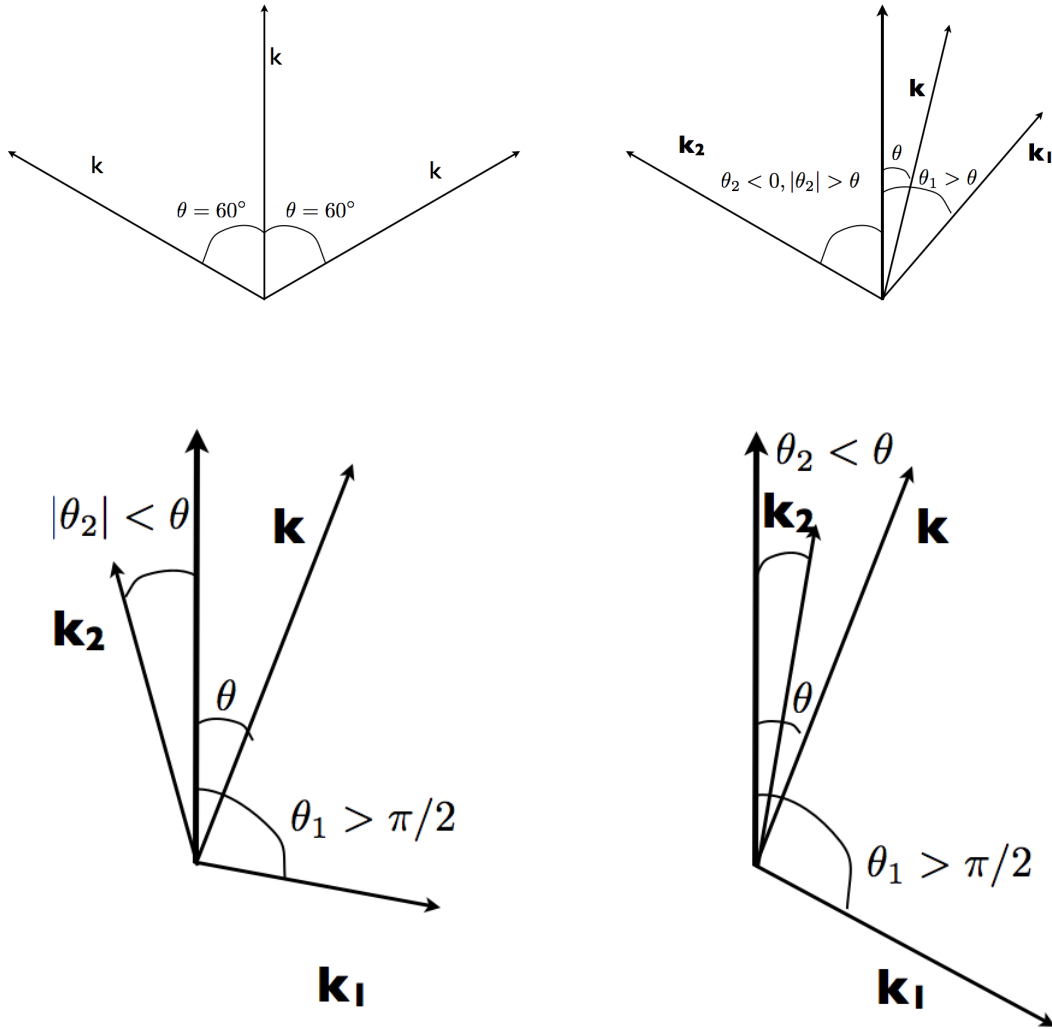


FIG. 3. Examples of wave decay. Parallel propagating into two oblique modes with  $k_1 = k_2 = k$ . Obliquely propagating into forward modes, Obliquely propagating into one backward propagating modes.

where

$$\delta \mathbf{B}_n = b_n \sqrt{\omega_n} \mathbf{e}_{B_n} e^{-i(\omega_n t - \mathbf{k}_n \cdot \mathbf{r})}, \quad n = \{0, 1, 2\} \quad (36)$$

[see 29, Eq. (2.1.3)].

The interaction matrix  $V$  takes an especially simple form for co-planar propagation in the  $x - y$

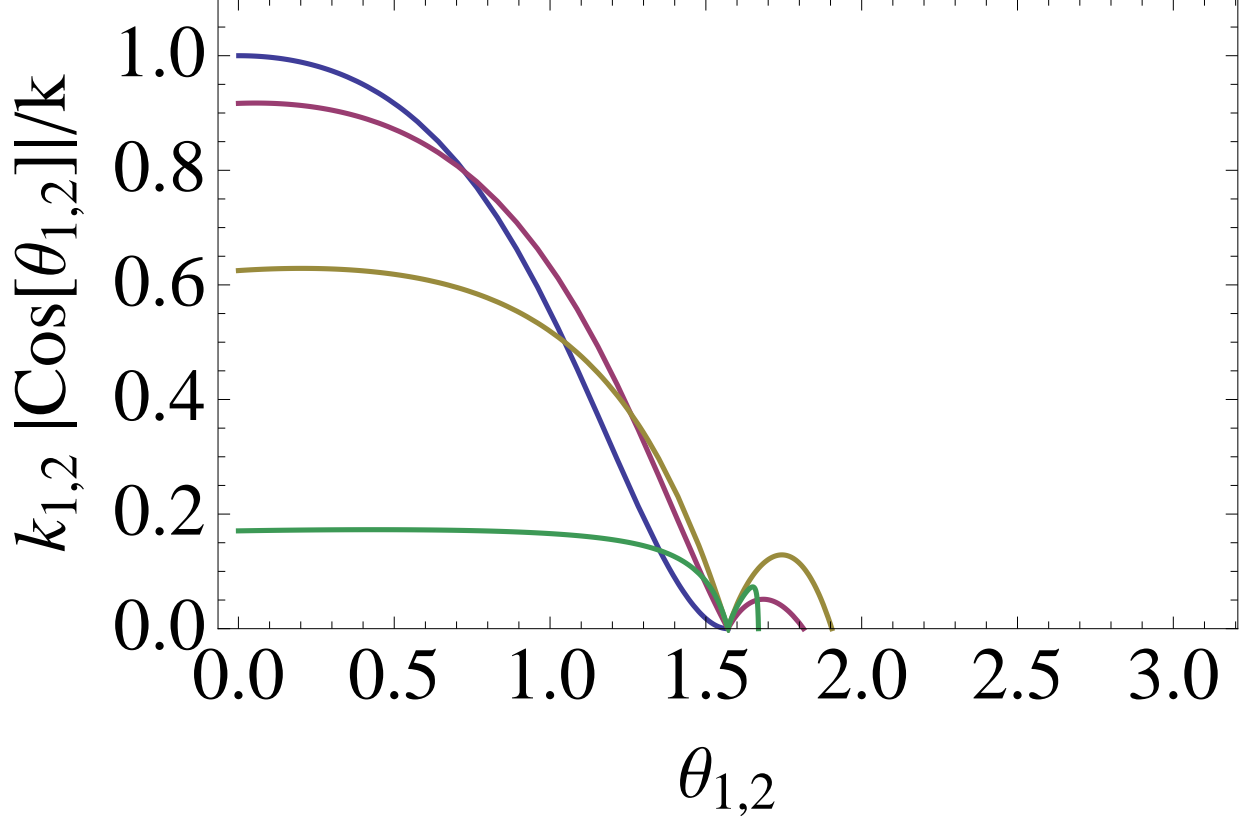


FIG. 4. Parallel wave vector for the decay modes (see Fig. 1 for notations). All daughter modes have  $k_{\parallel;1,2} < k$ .

plane. Setting  $\phi_n = 0$ ,

$$\begin{aligned}
 V_{0\leftrightarrow 1,2} &= \sqrt{\frac{\omega_1 \omega_2}{\omega_k}} \frac{k_1(k_2 - k_1)}{2\sqrt{2}} \cos^2 \frac{\theta - \theta_1}{2} \sin(\theta_1 - \theta_2) + (1 \leftrightarrow 2) = \\
 &\sqrt{\frac{\omega_1 \omega_2}{\omega_k}} \frac{k_1 - k_2}{2\sqrt{2}} (k_1(1 + \cos(\theta - \theta_1)) + k_2(1 + \cos(\theta - \theta_2))) \sin(\theta_1 - \theta_2). \quad (37)
 \end{aligned}$$

(For co-planar decay the angles  $\theta$  can be taken to vary between  $-\pi$  and  $\pi$ ).

The form of (37) clearly shows that decay into two co-linear modes (and merger of two co-linear modes),  $\theta_1 = \theta_2$ , is prohibited. More generally, the interaction highly disfavors decay into nearly aligned modes, as well as interaction of nearly aligned modes. The form of the interaction matrix  $V$  has important implications for the development of a turbulent cascade. Most importantly, whistler waves with highly different angles can experience a three-wave interaction.

For co-planar decay, for a given initial wave  $\{k, \theta\}$ , the interaction matrix depends only on one parameter (*e.g.*, the polar angle of one of the modes  $\theta_1$ ) - the other parameters can be eliminated using resonant conditions; explicit rations for  $k_{1,2}(\theta_{1,2})$  and  $\theta_2(\theta_1)$  were derived in Section VII A, see Fig. 6. For the decay of the wave that is initially propagating along magnetic field,  $\theta = 0$ , there is another property of the interaction matrix. As we discussed in Section II A, waves with  $k_1 = k_2$  and  $\theta_1 = \theta_2$  do not interact, or, alternatively, a decay into two such modes is prohibited.

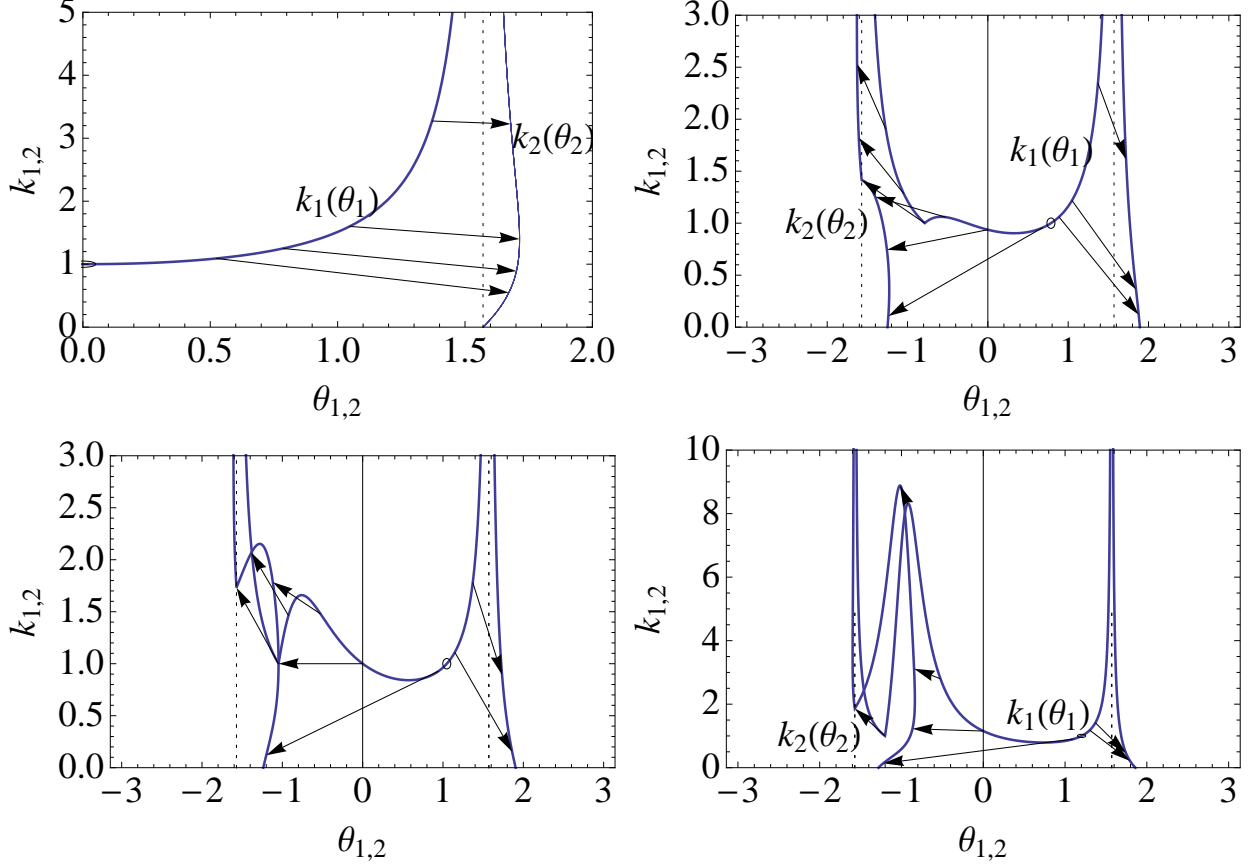


FIG. 5. Resonant condition for  $k; 1, 2$  interaction. *Upper Left Panel:*  $\theta = 0$ . Both daughter modes can have arbitrary large  $k_{1,2} \rightarrow \infty$  (for  $\theta_{1,2} \rightarrow \pi/2_{\pm 0}$ ), one of the modes propagates in the opposite direction,  $\theta_2 > \pi/2$ . For obliquely propagating parent wave  $\theta > 0$  (other panels) the resonant condition are very complicated even for co-planar propagation. For  $-\theta < \theta_1 < \theta$  the second mode has  $-\pi/2 < \theta_2 < 0$  (when  $\theta_1 \rightarrow -\theta_{+0}$ , then  $\theta_2 \rightarrow -\pi/2_{+0}$ ). For  $-\pi/2 < \theta_1 < -\theta$ , then  $\theta_2 < -\pi/2$ . The arrows connecting two daughter modes start at  $\{k_1, \theta_1\}$  and end at  $\{k_2, \theta_2\}$ . The two lower panels show that the resonant condition for  $k; 1, 2$  interaction is highly sensitive to  $\theta$ :  $\theta = 0.66 \times \pi/2$  for lower left panel and  $\theta = 0.765 \times \pi/2$  for lower right panel.

For the given three-wave interaction matrix (37) the kinetic equation reads [see 29, Eq. (2.1.12)].

$$\begin{aligned}
 \partial_t n &= \pi \int [ |V_{0\leftrightarrow 1,2}|^2 f_{k\leftrightarrow 1,2} \delta(\mathbf{k} - \mathbf{k}_1 - \mathbf{k}_2) \delta(\omega - \omega_1 - \omega_2) + \\
 & 2|V_{1\leftrightarrow k,2}| f_{1\leftrightarrow 0,2} \delta(\mathbf{k}_1 - \mathbf{k} - \mathbf{k}_2) \delta(\omega_1 - \omega - \omega_2) ] d\mathbf{k}_1 d\mathbf{k}_2 \\
 f_{0\leftrightarrow 1,2} &= n_1 n_2 - n(n_1 + n_2)
 \end{aligned} \tag{38}$$

## IX. KOLMOGOROV-LIKE WHISTLER CASCADE

### A. Anisotropy

Vainshtein probably was the first person to consider the EMHD turbulence [23]. His reasoning relied on what is now called the critically balanced cascade. This is now the most common approach to treat the EMHD cascade [8, 24–26]. Following the development of the MHD turbulence by [16], the MHD ideas of critical balance were transplanted to the EMHD turbulence. On the other hand,

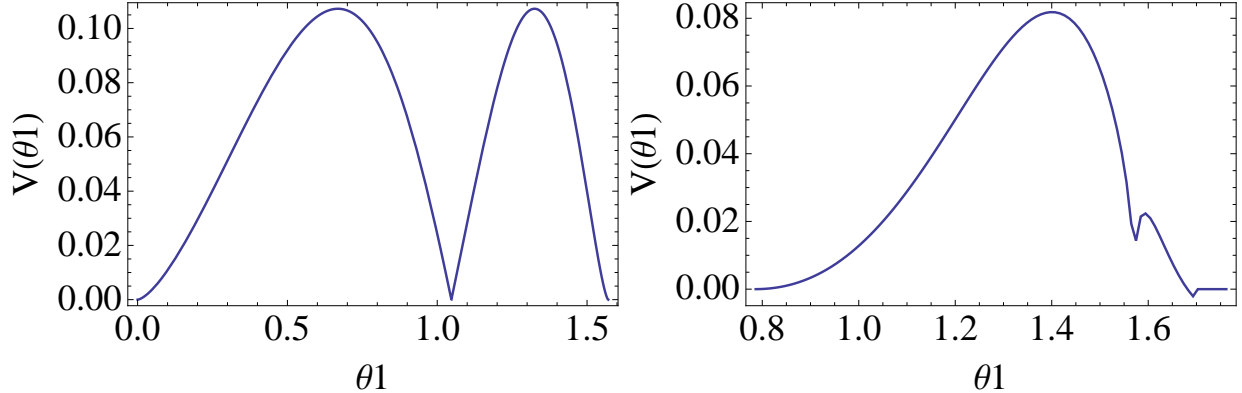


FIG. 6. *Left Panel.* Absolute value of the matrix element  $|V|$  for decay (37) for parallel propagating initial wave. Decay into two daughter modes with  $\theta = \pi/3$  (and  $k_1 = k_2$  is prohibited). *Right Panel.* Same for the propagation of the initial wave at  $\theta = \pi/4$ . The dip is at  $\theta_1 = \pi/2$ .

[2, 6] argued that the whistler turbulent cascade is isotropic and weak.

Above, we argued that the idea of the critically balanced cascade, based on the 4-mode interaction of non-dispersive Alfvén waves is not applicable to the EMHD cascade. On the other hand, a number of numerical simulations [*e.g.*, 25, 32, 33] seem to confirm the anisotropy, though the results of the numerical simulations regarding the spectrum remain controversial [27]. As we discuss below, observation of the highly anisotropic cascade in numerical simulations is likely to be an artifact of the limited dynamical and temporal range of simulations.

In Ref. [8] analytic arguments were suggested that the whistler cascade should be anisotropic. This was based on applying the Zakharov-Kuznetsov transformation [29] to the kinetic equation. Note, that generally, the matrix element for 3-wave whistler interaction is not a separable function of  $k_{\parallel}$  and  $\mathbf{k}_{\perp}$ , so that the Zakharov-Kuznetsov transformation cannot be achieved. In Ref. [8] it was first assumed that the turbulence is highly anisotropic, nearly transverse; in this limit the matrix element becomes separable in  $k_{\parallel}$  and  $\mathbf{k}_{\perp}$ , giving the scaling of the anisotropy cascade. In addition, the spectra suggested in Ref. [8] are not unique and IR divergent [34]; this further raises questions about their applicability. As we discuss below, the nature of the interaction matrix is such that it couples modes with very different propagation angles. As a result, in equipartition the angular distribution could be quasi-isotropic.

In astrophysical applications, for example, the EMHD cascade can occur in a collisionless plasma as a continuation of the MHD cascade. In Ref. [3] it was argued that the turbulent energy which is not damped on scales larger than the proton Larmor is transformed into whistlers and is eventually damped on electrons. Thus “stirring” at the largest EMHD scale is likely to be highly anisotropic, continuing the highly anisotropic criticality balance MHD cascade. Then two somewhat separate questions in relation to the anisotropy of the cascade arise. First is the temporal evolution of the cascade that is being stirred, possibly anisotropically, at the outer scale. Second is the asymptotic structure, when the cascade reached the inner scale (along all directions for the anisotropic case). As we argue below these two cases, time dependent and time asymptotic structure of the cascade imply very different spatial structure.

First note, that oblique mode decays preferentially into highly oblique, high  $k$  mode, (see Fig. 7). The daughter mode with  $k_{1,2} > k$  propagates at more oblique angles,  $\theta_{1,2} > \theta$ . Thus, each decay process will produce more oblique waves with higher  $k$ . On the other hand, the interaction of oblique whistler typically produce parallel modes with much smaller  $k$ . Thus, if there were no inverse process of wave merger and confluence, *a simple wave decay will lead to highly oblique modes with  $k \gg k_{inj}$ .*

Let us discuss the wave decay in more details. The suppression of the matrix element for highly oblique daughter waves,  $\propto \sqrt{\omega_{1,2}} \propto \sqrt{\cos \theta_{1,2}}$ , is partially compensated by large phase volume,  $\propto \theta_{1,2}$ . A single wave initially propagating along the magnetic field becomes nearly orthogonal within two decay cycles. For example, a parallel propagating mode has a decay probability peaking at  $\theta_{1,2} = 1.27$ . The secondary mode, propagating at  $\theta = 1.27$  has a decay probability peaking at  $\theta_{1,2} = 1.53$ , see Fig. 8. Thus, in the time-dependent case, if energy is injected at the outer scale of EMHD cascade, it will quickly within two interaction times become quasi-two-dimensional at  $k \gg k_{inj}$  just due to simple non-linear decay of whistler modes. By the nature of limited time evolution in numerical simulations, this is, we suggest, the origin of the anisotropy observed by a number of collaborations. It's a reflection of the fact that a simple non-linear whistler decay proceeds mostly in the perpendicular direction. On the other hand, at wave length not much larger than the injection, there is an inverse process of wave merging, that generally leads to the isotropization of the turbulence.

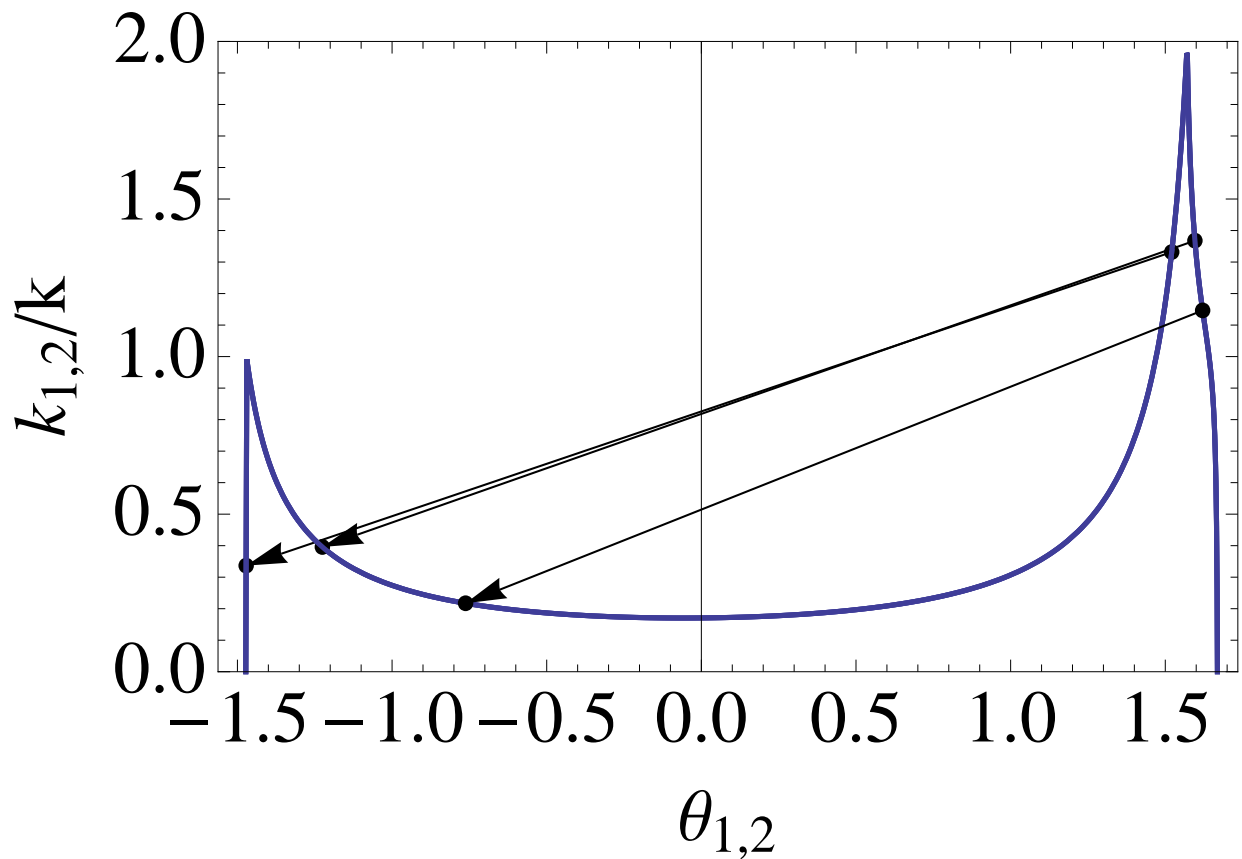


FIG. 7. Illustration that highly oblique whistlers decay preferentially into oblique whistlers, and that the interaction of two highly oblique whistlers produces a highly oblique whistler,  $\theta = \pi/2 - .1$ . For the product with small angle,  $\theta_{1,2} \rightarrow 0$ , the corresponding wave number is small.

Note, that *the whistler turbulence cannot become purely two dimensional*: for  $k_{\parallel} = 0$  the non-linear interaction freezes out: *any configuration  $B_z(x, y)$  satisfied the stationarity condition*. Thus, a cascade must develop in both directions, along the field and perpendicular. This also implies that the works which considered purely two dimensional EMHD turbulence need to be reconsidered.

The considerations given above are generally confirmed by numerical simulations, Section X, though a steep frequency dependence on the wave number, quickly increasing cascade rate and the apparent subtle dependence on the initial conditions prevent a decisive conclusion.



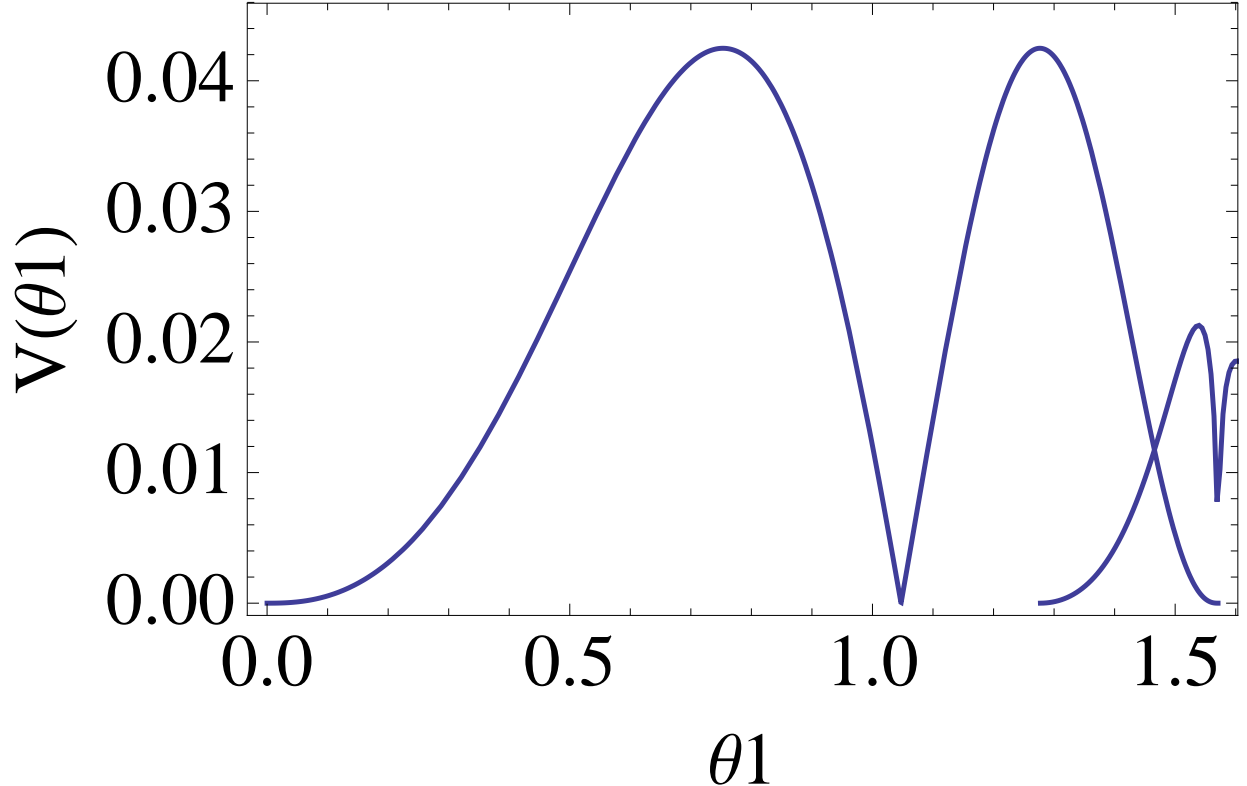


FIG. 8. Comparison of the decay matrix elements  $|V|$  for decay (37) for parallel propagating initial wave, and of the daughter wave emitted at maximum of  $V$ ,  $\theta_1 = 1.27$ . The most probable emission angle for the second generation decay product is within few percents of  $\pi/2$ .

Finally, we comment on the applicability of the reduced MHD approach to EMHD. For strong axial fields there is an often used approach called reduced MHD [35, 36], which allows considerable simplifications to the dynamic equations. Under reduced MHD approximation, the guiding magnetic field is assumed to be constant, while the fluctuations of the magnetic field are typically parametrized via the flux function  $P$ :  $\delta\mathbf{B}_\perp = \nabla(P) \times \mathbf{e}_x$ . This approach has also been applied to EMHD and closely related kinetic Alfvén wave turbulence, *e.g.*, Ref. [27, 33].

The reduced MHD approach is not applicable to EMHD. Whistlers are inherently three-dimensional structures: an obliquely propagating whistler mode produces field fluctuations in all directions, which are generally comparable in amplitude,  $\delta B_\parallel \sim \delta B_\perp$ . In fact, *a highly oblique mode produces large  $\delta B_\parallel$* , see Eq. (5). It is also easy to see that using the reduced MHD parametrization mentioned above the EMHD equations (3) cannot be satisfied.

## X. NUMERICAL SOLUTION OF THE KINETIC EQUATION

In this Section we numerically integrate Eq (38). We assume that at small wave numbers a large number of whistler modes is injected. We assume that the turbulence is back-forth symmetric, so that we can limit our integration to  $0 < \theta < \pi/2$  (if a wave with  $\theta > \pi/2$  is generated, it is then assumed that the counter propagating cascade generates a similar wave in the  $0 < \theta < \pi/2$  range).

Integration is done according to the following algorithm. For co-planar propagation three of the four integrations (over  $\{k_1, \theta_1\}$  and  $\{k_2, \theta_2\}$ ) are resolved using the resonance conditions (31-32). Special care should be taken to account for the allowed combinations of the resonant modes

and discarding the non-physical solutions, as described above. This leaves only integration over  $\sin \theta_1 d\theta_1$ . For a given  $\{k, \theta\}$  we sum is over all allowed  $\theta_1$  both for  $k; 12$  and  $1; k2$  processes. The time step is adjusted so that the relative variations of the occupation numbers at largest  $k$  be smaller than unity. Modes that fall into range  $k > k_{max}$  are removed. In addition, modes in the last  $\theta$ -cell are removed, as discussed above any  $B_x(y, z)$  is a solution of the stationary EMHD equation and thus do not participate in the cascade.

### A. Code validation

First note, that as we discussed in Section VII A, highly oblique low- $k$  modes can quickly create very high  $k$  modes. Keeping track of these high- $k$  modes is difficult, both due to their high wave-number (this puts constraint on the simulation domain) and due to the fact the interaction strength,  $\propto V^2$  grows as  $\sim k^6$ . As a result, at high  $k$  the cascade becomes very fast, so that at the upper limit on wave numbers the change in the occupation numbers becomes of the order of unity in one time step, possibly violating the assumed weak interaction, while it is still slow at low  $k$ . This is also related to the fact at sufficiently high  $k$  the cascade becomes explosive (see below). This puts a constraints on the integration time step. This, combined with the fact that even in the first generation the non-linear interaction produces very high  $k$  modes, does not allow to search numerically for a steady-state distribution.

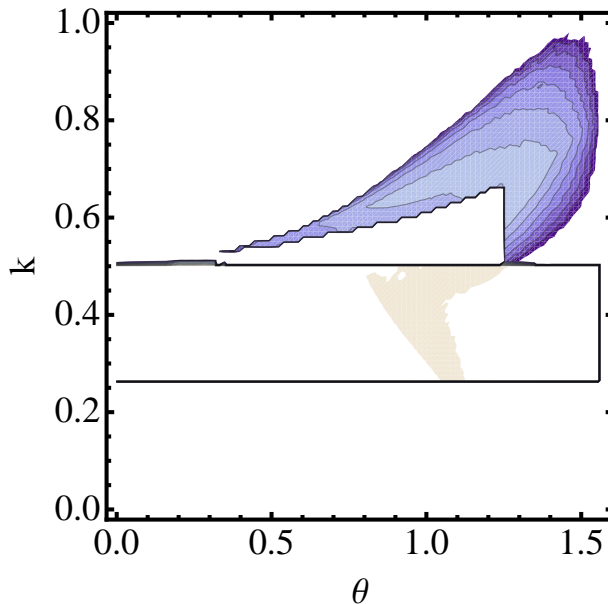


FIG. 9. Detailed simulation of the first generation spectrum close to the injection scale. Note that, first, at  $k \geq k_{inj}$  the spectrum is highly anisotropic. Often, this is a transient effect, see text for details.

### B. Results of the numerical solution of the kinetic equation

In this Section we discuss the results of the numerical solution of the kinetic equation. In the end we conclude that numerical integration confirm our analytical expectation: transiently, the wave decay leads to the formation of a highly oblique distribution at  $k > k_{inj}$ . Later, when a broad spectrum in  $k$  is present, the distribution can become a quasi-isotropic.

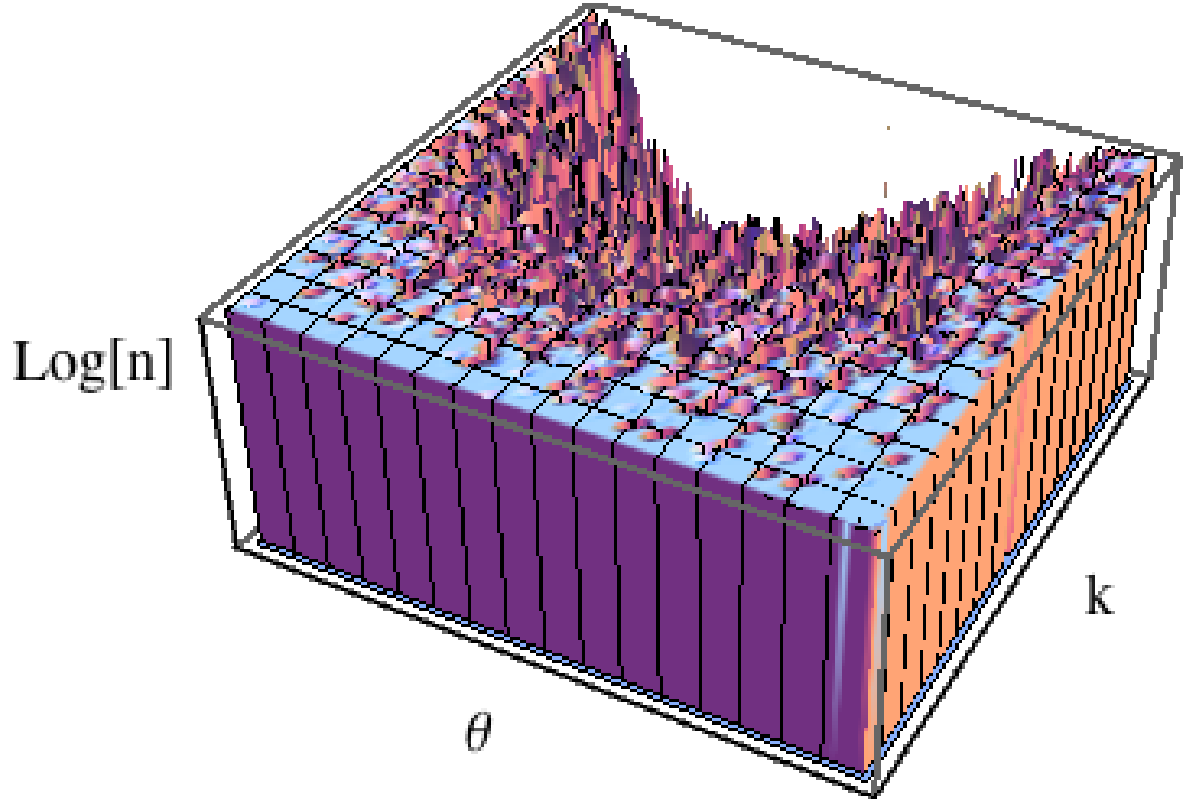


FIG. 10. Example of the non-linear evolution after one wave interaction. Initially, a constant number of waves per unit range of  $\theta$  and  $k$  is injected in the whole integration domain. The figure shows that higher  $k$  modes evolve much faster than the small  $k$  modes. This puts constraints on time integration and the overall range of the simulation. Due to complicated resonant conditions the wave interaction is intermittent, especially at small  $k$ . For injection homogeneous in  $k$  and  $\theta$  the modes are preferentially scattered out of small angles of propagation.

Generally, the simulations are highly dependent on the initial conditions. Depending on spectral properties of the injection (width in  $k$  and  $\theta$ ), behavior of the cascade can be drastically different. Generally broader injection results in faster cascade, while narrow injection may, under certain conditions, produce no cascade (within the integration limit). Injection spectra differing by a factor of a few in angular width could have dynamic time scales different by orders of magnitude. Injection spectra limited in  $\theta$  have strongly suppressed evolution and may not develop a cascade.

Due to complicated resonance conditions the spectra are highly intermittent in  $k$  and  $\theta$ ; the intermittency depends on the resolution. This is especially true at the edges of the integration domain, Fig. 10.

Let us discuss a number of calculations that concentrate on the first generations of the cascade development. Due to sensitive dependence of the interaction on the spectrum the time steps of the plotted examples are not equal - they are adjusted to display a typical interaction time scale.

Simulations of the broad angular injection spectrum are especially challenging: for sufficiently broad range of wave vectors even at first time step waves with the injection domain can interact leading to very high transfer rate, and putting very tight constraints on the integration time step.

First, we inject whistler modes in a limited range of wave number close to the lower limit of the calculation domain and consider various angular injection spectra: isotropic,  $\theta_{inj} < \pi/4$  and  $\theta_{inj} > 3\pi/4$ .

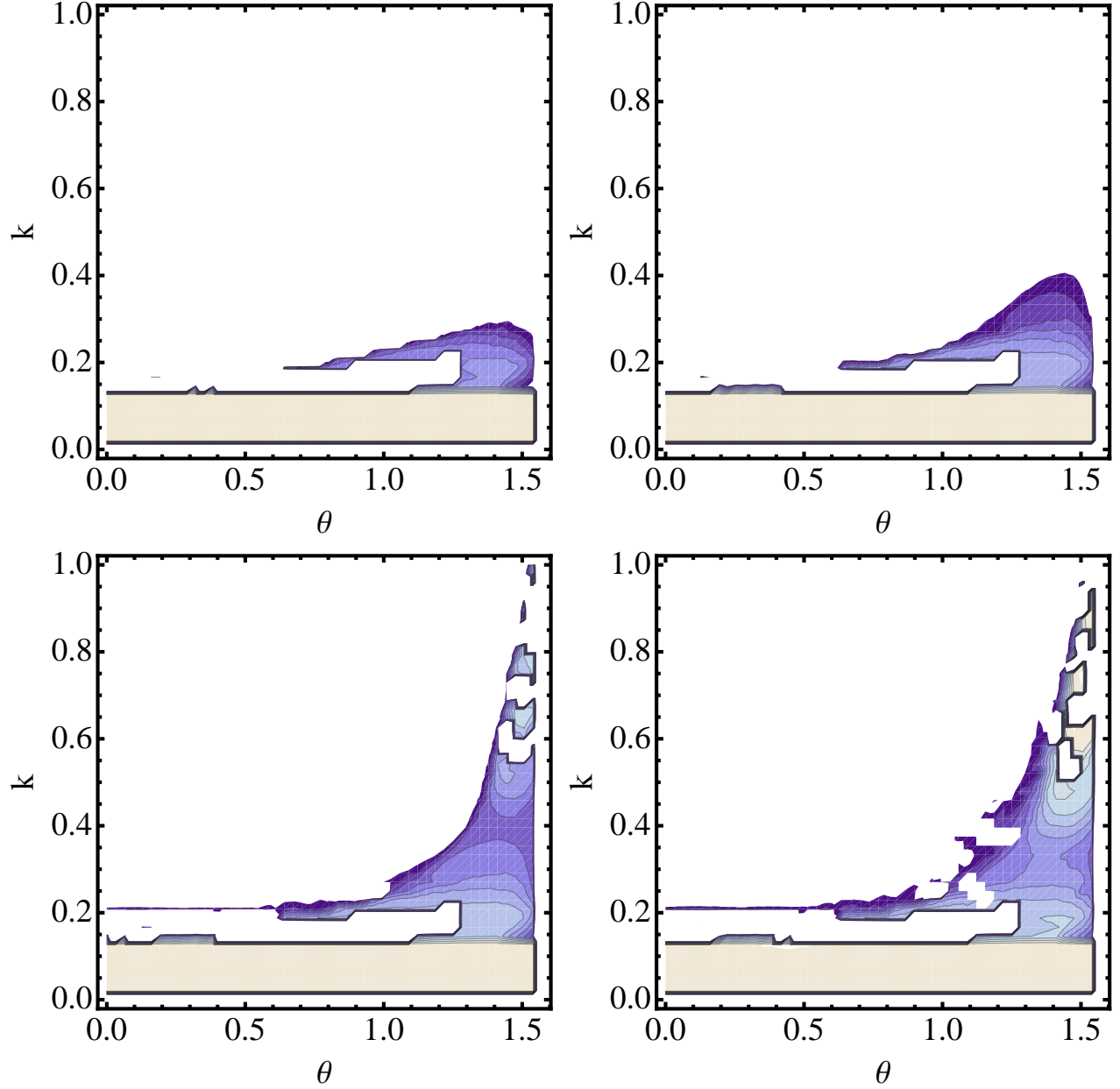


FIG. 11. Typical development of an initially isotropic cascade. Waves are injected with constant rate at small  $k_{inj}$ , at  $0 < \theta < \pi/2$  and are damped at  $k > 10$ . The spectrum reaches a steady state which is highly anisotropic.

As expected from the simple three-wave decay, Section VII, initially, at  $k > k_{inj}$  the spectrum is dominated by the decay products of the injected waves. Those decay products propagate preferentially at large angles to the magnetic field and may produce an impression of a highly anisotropic cascade. On the other hand, the second generation is nearly isotropic, presumably due to merger of two oblique waves of larger and/or similar  $k$ .

We also find that the development of the cascade is highly dependent on the details of the injected spectrum. For a given range of injected wave numbers  $k_{inj}$ , a broader injection spectrum in  $\theta$  would produce in the first generation more obliquely propagating waves. A spectrum limited in  $k$  and propagating at small  $\theta$  creates high- $\theta$  modes and vice versa, a spectrum limited to large

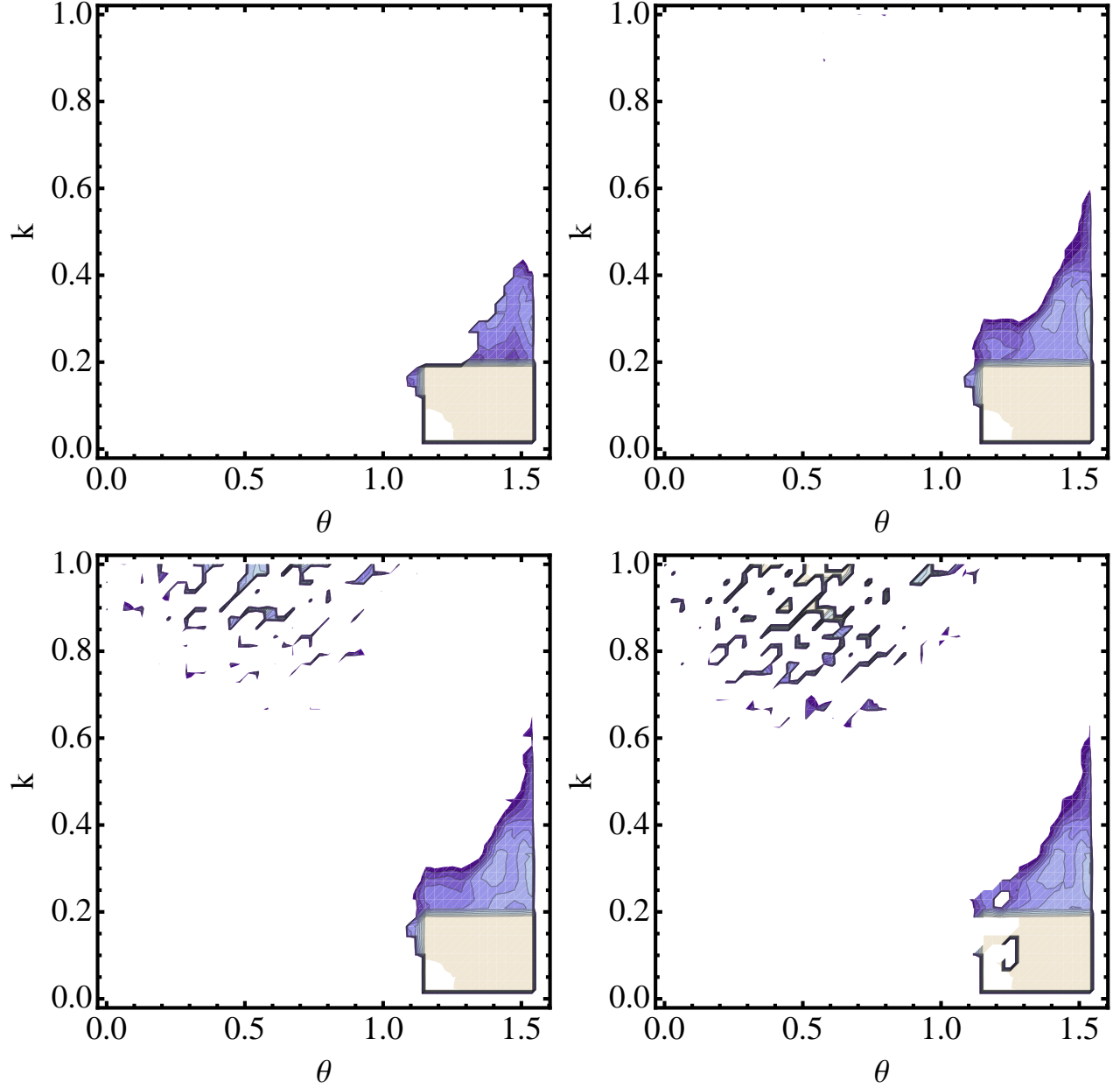


FIG. 12. Typical development of an initially quasi-perpendicular cascade. Waves are injected with constant rate at small  $k_{inj}$ , at  $\pi/4 < \theta < \pi/2$  and are damped at  $k > 100$ . The distribution at high- $k$  becomes parallel-enhanced.

$k$  create a broad, yet preferably parallel distribution, Fig. (12).

Based on a number of simulations runs we conclude that (i) given enough time the EMHD turbulence develops within a broad range of angles, *without* strong preference for perpendicular propagation; (ii) temporarily, especially for wave numbers not much larger than  $k_{inj}$  and for particular angular injection spectra, the cascade generally *does* develop high powers at large angles - but this is a transient effect; (iii) the development of a cascade is sensitive to the injection spectrum: for parallel-dominated injection the cascade *initially* develops slowly, yet given enough time a substantial perpendicular component is generated; (iv) the cascade efficiently couples high and small propagation angles, and creates in one integration time step very low and very high wave numbers;

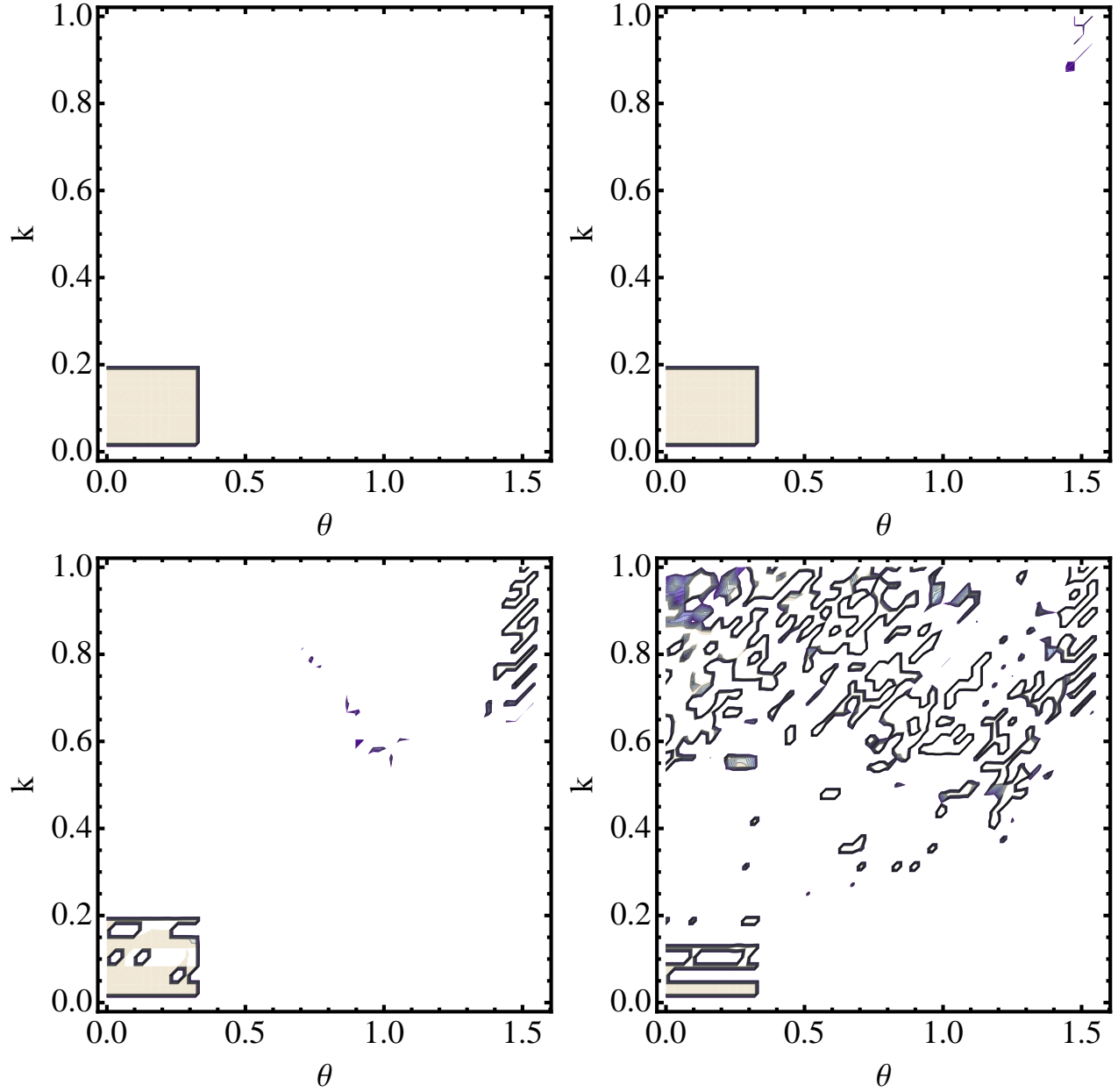


FIG. 13. Typical development of an initially quasi-parallel cascade. Waves are injected with constant rate at small  $k_{inj}$ , at  $0 < \theta < \pi/8$  and are damped at  $k > 10$ . Initially the cascade develops very slowly (integration time scale here is orders of magnitude longer than in Fig. 11), building a population of high- $\theta$  mode; after that the development is similar to the quasi-perpendicular injection: high- $\theta$  mode create a broad population of medium- $\theta$  modes. Plotted time steps are number 9,10,11,12 - at shorter times there is appreciable evolution while at the last time step the evolution become too quick to be captured by kinetic simulations.

(v) it is not clear if the cascade is stable: often the development of the cascade becomes explosive, quickly generating very large occupation numbers (and, thus violating the approximations used to derive the kinetic equation).

## XI. KOLMOGOROV-LIKE SPECTRUM OF WHISTLERS

### A. Spectrum

Above, in Section X, we argued that based on the numerical simulations EMHD is non-universal, the evolution of the cascade depends on the details of the forcing. Often, given enough time the EMHD turbulence develops within a broad range of angles, without strong preference for perpendicular propagation. The cascade cannot become truly isotropic, though.

Let us next estimate the parameters of the quasi-isotropic EMHD turbulence. Changing to occupation number presentations, on dimensional grounds,

$$\partial_t b \propto \frac{c}{ne} \sqrt{\omega} k^2 b^2 = V b^2 \quad (39)$$

where  $V$  is the 3-wave interaction coefficient. Thus, the interaction matrix  $V$  scales as

$$V \approx \frac{c}{ne} k^2 \sqrt{\omega} \propto k^3 \quad (40)$$

The interaction matrix  $V$  has the dimension  $cm^{1/2}g^{-1/2}s^{-1/2}$ , as it should [29].

Assuming locality in  $k$ -space and isotropy, the conservation of energy flux requires  $n_k \omega_k \nu_k = \text{constant}$ . The non-linear transfer rate [Eq. 2.1.13 of Ref. 29] is  $\nu_k \approx V^2 n_k / \omega_k$  where  $n_k$  is 1-D number density of the excitations. Using scalings of the matrix element,  $V \propto k^m$ ,  $m = 3$ , this gives

$$\begin{aligned} n_k &\propto k^{-m} \propto k^{-3} \\ \epsilon_k &= B_k^2 = \omega_k n_k \propto k^{-1} \\ \delta B_k &\propto k^{-1/2} \\ E_k &\propto \delta B_k^2 / k \propto k^{-2} \end{aligned} \quad (41)$$

where  $E_k$  is the spectral energy density of magnetic fluctuations.

Let us introduce Hall times on the outer scale  $L$

$$t_H = \frac{L^2 \omega_p^2}{c^2 \omega_B} \quad (42)$$

The non-linear transfer frequency is then

$$\nu_k t_H \sim (kL)^2 \frac{\delta B_k^2}{B_0^2} \quad (43)$$

where  $\delta B_k$  is a fluctuation at the scale  $L$ . This agrees with Ref. [6].

For this cascade scaling, the fluctuations of the magnetic field are

$$\delta B_k = \frac{\delta B_L}{\sqrt{kL}}, \quad (44)$$

while the non-linear transfer frequency is

$$\nu_k t_H = kL \frac{\delta B_L^2}{B_0^2} \quad (45)$$

If at the outer scales  $\delta B_L \sim B_0$ , then  $t_H \nu_k \sim kL \gg 1$  for  $k \gg 1/L$ . So, the largest eddy lives Hall time at largest scale, smaller eddies live shorter.

The cascade will be damped resistively on small scales. Taking resistivity into account the EMHD equation (3) becomes

$$\frac{\partial \mathbf{B}}{\partial t} = -\frac{c}{4\pi e} \nabla \times \left( \frac{\nabla \times \mathbf{B}}{n} \times \mathbf{B} \right) + \eta \Delta \mathbf{B} \quad (46)$$

where  $\eta$  is magnetic diffusivity. Let us introduce the Hall-Lundquist number  $S_H$  as the ratio of the linear dynamic to dissipative terms in Eq. (46)

$$S_H = \frac{\omega}{\eta k^2} = \frac{c^2 \omega_B}{\eta \omega_p^2} = \frac{L^2}{\eta t_H} \quad (47)$$

In Ref. [6] this parameter was called  $\mathcal{R}_B$  and it was argued that for  $S_H \gg 1$  the Hall plasma evolves through a turbulent cascade with inertial range. Note, that unlike the case of viscous fluid and resistive MHD, *the ratio of the linear dynamic to resistive terms is scale-independent* in EMHD.

On the other hand, the non-linear and resistive time scale become comparable at

$$\frac{L_{\text{res}}}{L} = \frac{1}{S_H} \frac{B_0^2}{\delta B_L^2} \quad (48)$$

Thus, for  $\delta B_L \sim B_0$  and  $S_H \gg 1$  there is a separation of cascade scales, and there is an inertial range. This requires that the magnetic diffusivity satisfies

$$\eta < \eta_{\text{crit}} = \frac{c^2 \omega_B}{\omega_p^2} \frac{\delta B_L^2}{B_0^2} \quad (49)$$

## B. Locality and strength of the quasi-isotropic EMHD Kolmogorov-like spectrum

In the thermodynamic equilibrium we expect  $n_k \propto T/\omega_k \propto k^{-2}$ , while in the EMHD cascade  $n_k \propto T/\omega_k \propto k^{-3}$ ; thus, the energy in the cascade will go to larger  $k$  - whistlers obey a direct energy cascade.

Kolmogorov-type cascades require locality, that the interaction integral converges. Assuming that  $k_1 \ll k, k_2$ , the interaction matrix of whistler waves scales as

$$V \propto k_1^{m_1} k^{m-m_1}, m_1 = 1, m = 3 \quad (50)$$

(For whistlers,  $V \propto (k_1 k_2/k) \times (k_1 \text{ or } k_2)$ ). Infrared locality requires [29]  $z_{IR} = 2m_1 - m + 1 > 0$ . In our case  $z_{IR} = 0$ , thus, the infrared locality is weakly violated (see also Ref. [34]). Since the infrared locality is violated, this has important implication for transfer of energy to large scales and for the overall existence of the steady universal Kolmogorov-like spectrum.

Ultraviolet locality, in the limit  $k_{1,2} \gg k$  of the 3-wave interaction requires  $(\omega \propto k^\alpha) z_{UV} = 2m_1 - m + \alpha > 0$ . In our case  $\alpha = 2$ ,  $m_1 = 1$  or  $m_1 = 2$ , in the limit  $k_{1,2} \gg k$ ,  $V \propto k_1^2 k_2^2 k^{-1}$ , so that  $z_{UV} = 3 > 0$ : that the ultraviolet locality is satisfied.

We can also compare the non-linear time scale with the wave frequency

$$\frac{\nu_k}{\omega_k} = \frac{\delta B_k^2}{B_0^2} = \frac{1}{kL} \frac{\delta B_L^2}{B_0^2} \leq 1 \quad (51)$$

Thus, the cascade becomes weaker for larger  $k$ . This is consistent with the general condition for the weak cascade. Comparing intensities of 3-wave and 4-waves interaction, for  $\alpha > (5-d)/3$  the turbulence is weak for large  $k$  [29]. In our case  $\alpha = 2 > 2/3$ , the turbulence is weaker at larger



$k$ . Thus, *whistler cascade becomes weaker for large  $k$* . Since these estimates come from comparing intensities of 3-wave and 4-waves interaction, they are inapplicable to the Alfvén MHD turbulence.

Note, that the cascade accelerates towards small scales, becoming explosive. A wave number of a perturbation with the initial  $k \sim 1/L$  evolves according to ( $\partial_t k = \nu_k k$ ,  $\nu_k$  is given by Eq. (45)),

$$k(t) = \left(1 - \frac{t}{t_H} \frac{\delta B_L^2}{B_0^2}\right)^{-1} \frac{1}{L} \quad (52)$$

Thus, there is accelerating, explosive transfer on time scale

$$t_{casc} \sim t_H \frac{B_0^2}{\delta B_L^2} \quad (53)$$

Though the cascade develops explosively, at each  $k$  the non-linear interaction time remains smaller than the wave frequency, so the cascade, formally, remains weak. The fact that the cascade develops very fast at high  $k$  makes the investigation of the time-asymptotic structure and the stability very challenging. We expect that at high wave numbers other physical effects, like resistivity and electron inertial would become important and resolve the formal singularity in Eq. (52)

### C. Localized resistive heating

For magnetic field (44) the fluctuations of the current increase with  $k$ :

$$\delta J = \frac{4\pi}{c} \delta B_L \sqrt{\frac{k}{L}} \quad (54)$$

The resistive heating is then (in ergs  $\text{cm}^{-3} \text{s}^{-1}$ )

$$\dot{\epsilon} = \eta J^2 = \eta \delta B_L^2 \frac{k}{L} \quad (55)$$

At the inner scale the dissipation rate is

$$\dot{\epsilon}_{\text{res}} = \frac{\delta B_L^4}{B_0^2 t_H} = \frac{\delta B_L^2}{t_{casc}} \quad (56)$$

(so that all the cascade energy is dissipated on the cascade time scale).

Localized resistive dissipation will be balanced by heat conduction. Since the thermal conduction flux  $\propto k$ , the ratio of heating (Eq. (55)) to cooling is independent of  $k$ . In most applications the thermal conduction times are much shorter than the Hall time, so that the localized dissipation by the EMHD cascade is likely not to be important.

## XII. CONCLUSION

In this paper we studied the plasma dynamics and turbulence in the particular regime of inertialess electron MHD. Our main result is that analogies with the Alfvén turbulence cannot be transferred to the EMHD turbulence. First, there is no energy principle in EMHD: an arbitrary EMHD configuration does not first settle to a preferred state and then decay slowly, like an MHD plasma does. Instead, EMHD behaves similarly to the incompressible fluid, dissipating energy via the turbulent cascade.

We considered in detail the three-wave interaction of whistlers and argued that it is very different from the MHD case: (i) in EMHD *only harmonic* whistlers are exact (non-linear) solutions; (ii) co-linear whistlers do not interact; (iii) whistler modes with very different  $k$  and  $\theta$  can interact resonantly, via three-wave coupling, including those with zero frequency wave. Such processes are allowed both kinematically (the resonance condition is satisfied), as well dynamically (non-vanishing interaction matrix). We argue that such strong coupling between waves propagating at different angles would in the general case eventually prevent a formation of highly anisotropic spectrum.

We have solved numerically the wave kinetic equation for various injection spectra. We found that the results of the simulations are highly dependent on the injection spectrum and on the numerical details. Often, as time progresses the spectrum becomes quasi-isotropic. On the other hand, *transiently* the cascade does develop highly anisotropic structures and suggest that a number of numerical simulations did catch this transient effect. Note that the fact that the cascade becomes very fast at wave numbers exceeding the injection scale, by a factor as high as  $k^6$  (and, actually, accelerating) makes it numerically challenging even for simple kinetic simulations that we adopted.

Thus, using analytical and numerical calculations we argue that the EMHD turbulence may become quasi-isotropic, in a sense that it is not limited to a narrow range of angles, but may still behave broadly anisotropic. Based on this, and the scaling of the interaction matrix, we find that the stationary whistler turbulence should obey a  $k^{-2}$  spectrums, as initially suggested in Ref. [6]. On the other hand, the fact that the transfer rate becomes explosive and that the spectrum shows a IR divergence raises the questions about the stability and universality of this spectrum.

The key limitation of our approach is the assumption of constant underlying density. It is well known [2, 37] that density gradients lead to whistler drifts that may lead to the formation of current sheets approximately in one Hall time. Formation of current sheets may have important implications for the behavior of the magnetic field. We will incorporate the density drifts in a future work.

I would like to thank Stanislav Boldyrev, Jungyeon Cho, Perter Goldreich, Alexander Lazarian, and Christopher Thompson for numerous enlightening discussions. This research was partially supported by NASA grants NNX12AO85G, NNX12AF92G and by the Simons Foundation.

- 
- [1] M. J. Lighthill, Royal Society of London Philosophical Transactions Series A **252**, 397 (1960).
  - [2] A. S. Kingsep, K. V. Chukbar, and V. V. Ian'kov, Voprosy Teorii Plazmy **16**, 209 (1987).
  - [3] E. Quataert and A. Gruzinov, ApJ **520**, 248 (1999), arXiv:astro-ph/9803112.
  - [4] C. H. K. Chen, S. Boldyrev, Q. Xia, and J. C. Perez, Physical Review Letters **110**, 225002 (2013), 1305.2950.
  - [5] C. Thompson and R. C. Duncan, ApJ **408**, 194 (1993).
  - [6] P. Goldreich and A. Reisenegger, ApJ **395**, 250 (1992).
  - [7] V. I. Arnold, *Mathematical methods of classical mechanics* (1978).
  - [8] S. Galtier and A. Bhattacharjee, Physics of Plasmas **10**, 3065 (2003).
  - [9] I. B. Bernstein, E. A. Frieman, M. D. Kruskal, and R. M. Kulsrud, Royal Society of London Proceedings Series A **244**, 17 (1958).
  - [10] L. Woltjer, ApJ **128**, 384 (1958).
  - [11] R. J. Tayler, MNRAS **162**, 17 (1973).
  - [12] R. M. Kulsrud, *Plasma physics for astrophysics* (Princeton, N.J. : Princeton University Press, c2005. (Princeton series in astrophysics), 2005).
  - [13] H. Lamb, *Hydrodynamics* (Cambridge: Cambridge University Press, 1975, 6th ed., 1975).
  - [14] P. S. Iroshnikov, AZh **40**, 742 (1963).
  - [15] R. H. Kraichnan, Physics of Fluids **8**, 1385 (1965).
  - [16] S. Sridhar and P. Goldreich, ApJ **432**, 612 (1994).
  - [17] P. Goldreich and S. Sridhar, ApJ **438**, 763 (1995).

- [18] P. Goldreich and S. Sridhar, ApJ **485**, 680 (1997), arXiv:astro-ph/9612243.
- [19] J. V. Shebalin, W. H. Matthaeus, and D. Montgomery, Journal of Plasma Physics **29**, 525 (1983).
- [20] D. Montgomery and W. H. Matthaeus, ApJ **447**, 706 (1995).
- [21] C. S. Ng and A. Bhattacharjee, ApJ **465**, 845 (1996).
- [22] S. Boldyrev, Physical Review Letters **96**, 115002 (2006), arXiv:astro-ph/0511290.
- [23] S. I. Vainshtein, Soviet Journal of Experimental and Theoretical Physics **37**, 73 (1973).
- [24] D. Biskamp, E. Schwarz, A. Zeiler, A. Celani, and J. F. Drake, Physics of Plasmas **6**, 751 (1999).
- [25] J. Cho and A. Lazarian, ApJ **615**, L41 (2004), arXiv:astro-ph/0406595.
- [26] G. G. Howes, W. Dorland, S. C. Cowley, G. W. Hammett, E. Quataert, A. A. Schekochihin, and T. Tatsuno, Physical Review Letters **100**, 065004 (2008), 0711.4355.
- [27] S. Boldyrev and J. C. Perez, ApJ **758**, L44 (2012), 1204.5809.
- [28] V. E. Zakharov and E. A. Kuznetsov, Physics Uspekhi **40**, 1087 (1997).
- [29] V. E. Zakharov, V. S. L'Vov, and G. Falkovich, *Kolmogorov spectra of turbulence I: Wave turbulence* (Springer Series in Nonlinear Dynamics, Berlin: Springer, 1992, 1992).
- [30] N. Bogolyubov and D. Shirkov (1988).
- [31] L. H. Ryder, *Quantum Field Theory* (1996).
- [32] J. Cho and A. Lazarian, ApJ **701**, 236 (2009), 0904.0661.
- [33] J. M. TenBarge and G. G. Howes, Physics of Plasmas **19**, 055901 (2012).
- [34] S. Boldyrev, Bulletin Lebedev Phys. Institute (Allerton Press, New York) **1**, 1 (1995).
- [35] G. P. Zank and W. H. Matthaeus, Journal of Plasma Physics **48**, 85 (1992).
- [36] D. Biskamp, *Nonlinear Magnetohydrodynamics* (1997).
- [37] A. V. Gordeev, A. S. Kingsep, and L. I. Rudakov, Phys. Rep. **243**, 215 (1994).
- [38] N. McLachlan, *Theory and Application of Mathieu Functions* (Oxford University Press, 1947).

### Appendix A: Interaction of zero frequency mode and whistlers: parametric instability

In a complementary approach, let us consider interaction of a single transverse zero frequency mode, with the wave vector orthogonal to the magnetic field, and an oblique whistler waves. The background field is  $B_x(y, z)$ ; such structure still satisfied the stationary condition  $\nabla \times (\nabla \times \mathbf{B} \times \mathbf{B}) = 0$ . For simplicity, let us assume  $B_x = B_0 + \delta B_0 \cos(k_0 y)$ . Let us then impose whistler perturbations  $\delta \mathbf{B} = \{\delta B_x, \delta B_y, \delta B_z\} e^{-i(\omega t - k_x x)}$ . Using the  $\text{div } \mathbf{B} = 0$  condition and assuming small initial perturbations  $\delta B_y/B_0 \ll 1$ , we find

$$\frac{\delta B_y''}{\delta B_y} = k_x^2 - \frac{\omega^2}{B_0^2 k_x^2} - \left( k_0^2 - 2 \frac{\omega^2}{B_0^2 k_x^2} \right) \frac{\delta B_y}{B_0} \cos(k_0 y) \quad (\text{A1})$$

where prime denotes differentiation with respect to  $y$ . For small frequencies,  $\omega \ll B_0 k_x^2$ , this equation reduces to Mathieu's equation,

$$\frac{\delta B_y''}{\delta B_y} = k_x^2 - k_0^2 \frac{\delta B_y}{B_0} \cos(k_0 y) \quad (\text{A2})$$

Mathieu's equation (A2) is well known in mathematical physics [38]. It has solutions which show instability bands centered (for small amplitude of modulation  $\delta B_y/B_0 \ll 1$ ) on  $k_x^2 = k_0^2 m/2$ , where  $m$  is integer. Thus, for a given periodic transverse variations with the wave number  $k$ , there are whistler modes that would produce exponentially growing magnetic field (as functions of  $y$ ). Importantly, the effect is *linear* in the amplitude of the whistler mode: regardless of the strength of the wave it can lead to the creation of divergent magnetic field structures. These structures are created on scales of the order of the scale of the magnetic field inhomogeneity. Temporarily, they will be created on a whistler time scale. The fact that the parametric instability is linear in the amplitude of the wave and that it can operate in a constant density background distinguishes it from the non-linear Burger-type instability in the density gradient [2].

An important limitation of the above approach is that it assumes that there exists *a single* zero frequency mode. For the parametric instability it is required that the waves keep coherence over long temporal and/or spacial scales. Presence of other modes will destroy such coherence.